Supersymmetric electroweak corrections to heavier top squark decay into a lighter top squark and neutral Higgs boson

Qiang Li, Li Gang Jin, and Chong Sheng Li
Department of Physics, Peking University, Beijing 100871, People's Republic of China
(Received 30 July 2002; published 30 December 2002)

We calculate the Yukawa corrections of order $\mathcal{O}(\alpha_{ew}m_{t(b)}^2/m_W^2)$, $\mathcal{O}(\alpha_{ew}m_{t(b)}^3/m_W^3)$, and $\mathcal{O}(\alpha_{ew}m_{t(b)}^4/m_W^4)$ to the widths of the decays $\tilde{t}_2\to\tilde{t}_1+(h^0,H^0,A^0)$ in the minimal supersymmetric standard model, and perform a detailed numerical analysis. We also compare the results with the ones presented in earlier literature, where the $\mathcal{O}(\alpha_s)$ supersymmetric (SUSY) QCD corrections to the same three decay processes have been calculated. Our numerical results show that, for the decays $\tilde{t}_2\to\tilde{t}_1+h^0$, $\tilde{t}_2\to\tilde{t}_1+H^0$, the Yukawa corrections are significant in most of the parameter range, and can reach approximately 10%; for the decay $\tilde{t}_2\to\tilde{t}_1+A^0$, the Yukawa corrections are smaller, only a few percent. The numerical calculations also show that using the running quark masses and the running trilinear coupling A_t, including the QCD, SUSY QCD, and SUSY-electroweak effects, and resumming all high order $(\tan\beta)$-enhanced effects, can vastly improve the convergence of the perturbation expansion. We also discuss the effects of the running of the Higgsino mass parameter μ on the corrections, and find that they are significant, too, especially for large $\tan\beta$.

DOI: 10.1103/PhysRevD.66.115008 PACS number(s): 14.80.Ly, 12.38.Bx, 14.80.Cp

I. INTRODUCTION

The incorporation of supersymmetry is one of the most attractive and promising possibilities for new physics beyond the standard model (SM) [1,2], and the minimal supersymmetric standard model (MSSM) is a popular candidate for new physics in this way. In the MSSM there are many new particles. For example, every quark has two spin zero partners called squarks, $\tilde{q}_L$ and $\tilde{q}_R$, one for each chirality eigenstate, which mix to form the mass eigenstates $\tilde{q}_1$ and $\tilde{q}_2$. For the third generation quarks, due to large Yukawa couplings, there may be large mass differences between the lighter mass eigenstate and the heavier one, which implies in general a very complex decay pattern of the heavier state.

As we know, the next generation of colliders, such as the CERN Large Hadron Collider (LHC), the upgraded Fermilab Tevatron, e^+e^- linear colliders, and $\mu^+\mu^-$ colliders will push the discovery reach for supersymmetric (SUSY) particles with masses up to 2.5 TeV [3,4] and allow for precise measurement of the MSSM parameters. Thus more accurate calculations of the decay mechanisms beyond the tree level are necessary. The dominate decay modes of the heavier squarks are shown below:

$$\tilde{t}_i\to t\tilde{\chi}^0_k, b\tilde{\chi}^+_k;\quad \tilde{b}_i\to b\tilde{\chi}^0_k, t\tilde{\chi}^+_k;\quad \tilde{t}_i\to t\tilde{g};\quad \tilde{b}_i\to b\tilde{g};$$

$$\tilde{t}_2\to\tilde{t}_1Z^0;\quad \tilde{t}_i\to\tilde{b}_jW^+;\quad \tilde{b}_2\to\tilde{b}_1Z^0;\quad \tilde{b}_i\to\tilde{t}_jW^-;$$

$$\tilde{b}_i\to\tilde{t}_jH^-;\quad \tilde{t}_i\to\tilde{b}_jH^+;\quad \tilde{t}_2\to\tilde{t}_1(h^0,H^0,A^0).$$

All these squark decays have been extensively discussed at the tree level [5–7]. Up to now, one-loop QCD and supersymmetric QCD corrections to the above decay channels have also been calculated [6,8,9], while the Yukawa corrections and the full electroweak one-loop radiative corrections to the squark decays into quarks plus charginos and neutralinos were given in Ref. [10] and Ref. [11], respectively. In addition, the Yukawa corrections to the squark decays into quarks plus gluinos were given in Refs. [12,13], and the Yukawa corrections to the heavier squark decays into lighter squarks plus vector bosons were given in Ref. [14]. Recently, the Yukawa corrections to the bottom squark decays into lighter top squarks plus charged Higgs bosons were presented in Ref. [15]. Thus only the electroweak radiative corrections to the heavier top squark decays into lighter top squarks plus neutral Higgs bosons have not been calculated yet, including the Yukawa corrections to these processes.

In this paper, we present the calculations of the Yukawa corrections of order $\mathcal{O}(\alpha_{ew}m_{t(b)}^2/m_W^2)$, $\mathcal{O}(\alpha_{ew}m_{t(b)}^3/m_W^3)$, and $\mathcal{O}(\alpha_{ew}m_{t(b)}^4/m_W^4)$ to the widths of the heavier top squark decays into lighter top squarks plus neutral Higgs bosons, i.e., the decays $\tilde{t}_2\to\tilde{t}_1+(h^0,H^0,A^0)$. These corrections are mainly induced by the Yukawa couplings from Higgs-quark-quark couplings, Higgs-squark-squark couplings, Higgs-Higgs-squark-squark couplings, chargino- (neutralino)-quark-squark couplings, and squark-squark-squark-squark couplings. As shown in Ref. [16], the Higgs-squark-squark couplings receive large radiative corrections, which can make the perturbation calculation of the relevant squark or Higgs boson decay widths quite unreliable in some region of the parameter space. When the correction term is negative, the corrected width can even become negative, which clearly makes no sense. In order to solve this problem, we use running quark masses and running trilinear coupling A_t [16], and vastly improve the convergence of the perturbation expansion. We also discuss the effects of the running of the Higgsino mass parameter μ on the corrections, and find that they are also significant, especially for large $\tan\beta$.

II. NOTATION AND TREE-LEVEL RESULT

In order to make this paper self-contained, we first summarize our notation and present the relevant interaction

Lagrangians of the MSSM and the tree-level decay rates for $\tilde{t}_2 \to \tilde{t}_1 + (h^0, H^0, A^0)$.

The current eigenstates $\tilde{q}_L$ and $\tilde{q}_R$ are related to the mass eigenstates $\tilde{q}_1$ and $\tilde{q}_2$ by

$$\begin{pmatrix} \tilde{q}_1 \\ \tilde{q}_2 \end{pmatrix} = R^{\tilde{q}} \begin{pmatrix} \tilde{q}_L \\ \tilde{q}_R \end{pmatrix}, \quad R^{\tilde{q}} = \begin{pmatrix} \cos\theta_{\tilde{q}} & \sin\theta_{\tilde{q}} \\ -\sin\theta_{\tilde{q}} & \cos\theta_{\tilde{q}} \end{pmatrix} \tag{1}$$

with $0 \leqslant \theta_{\tilde{q}} < \pi$ by convention. Correspondingly, the mass eigenvalues $m_{\tilde{q}_1}$ and $m_{\tilde{q}_2}$ (with $m_{\tilde{q}_1} \leqslant m_{\tilde{q}_2}$) are given by

$$\begin{pmatrix} m^2_{\tilde{q}_1} & 0 \\ 0 & m^2_{\tilde{q}_2} \end{pmatrix} = R^{\tilde{q}} M^2_{\tilde{q}} (R^{\tilde{q}})^\dagger, \quad M^2_{\tilde{q}} = \begin{pmatrix} m^2_{\tilde{q}_L} & a_q m_q \\ a_q m_q & m^2_{\tilde{q}_R} \end{pmatrix} \tag{2}$$

with

$$m^2_{\tilde{q}_L} = M^2_{\tilde{Q}} + m_q^2 + m_Z^2 \cos 2\beta (I^q_{3L} - e_q \sin^2\theta_W), \tag{3}$$

$$m^2_{\tilde{q}_R} = M^2_{\{\tilde{U},\tilde{D}\}} + m_q^2 + m_Z^2 \cos 2\beta e_q \sin^2\theta_W, \tag{4}$$

$$a_q = A_q - \mu\{\cot\beta, \tan\beta\} \tag{5}$$

for {up, down} type squarks. Here $M^2_{\tilde{q}}$ is the squark mass matrix. $M_{\tilde{Q},\tilde{U},\tilde{D}}$ and $A_{t,b}$ are soft SUSY-breaking parameters and μ is the Higgsino mass parameter. I^q_{3L} and e_q are the third component of the weak isospin and the electric charge of the quark q, respectively.

Defining $H_k = (h^0, H^0, A^0, G^0, H^\pm, G^\pm)(k=1,\ldots,6)$, one can write the relevant Lagrangian density in the $(\tilde{q}_1, \tilde{q}_2)$ basis as $(i,j=1,2;$ α and β are flavor indices)

$$\begin{aligned} \mathcal{L}_{\text{relevant}} = {} & H_k \overline{q^\beta} (a_k^\alpha P_L + b_k^\alpha P_R) q^\alpha + (G_k^{\tilde{\alpha}})_{ij} H_k \tilde{q}_j^{\beta *} \tilde{q}_i^\alpha \\ & + g \overline{q} (a_{ik}^{\tilde{q}} P_R + b_{ik}^{\tilde{q}}) \tilde{\chi}_k^0 \tilde{q}_i + g \overline{t} (l_{ik}^{\tilde{b}} P_R + k_{ik}^{\tilde{b}} P_L) \tilde{\chi}_k^+ \tilde{b}_i \\ & + g \overline{b} (l_{ik}^{\tilde{t}} P_R + k_{ik}^{\tilde{t}} P_L) \tilde{\chi}_k^{+c} \tilde{t}_i + (G_{lk}^{\tilde{\alpha}})_{ij} H_l H_k \tilde{q}_j^{\beta *} \tilde{q}_i^\alpha \\ & + \text{H.c.}, \end{aligned} \tag{6}$$

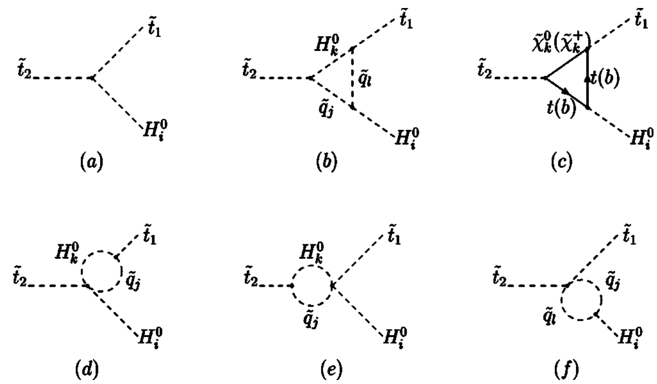

FIG. 1. Feynman diagrams contributing to supersymmetric electroweak corrections to $\tilde{t}_2 \to \tilde{t}_1 H_i^0$: H_i^0, $i=1,2,3$ correspond to h^0, H^0, A^0. (a) Tree-level diagram; (b)–(f) are one-loop vertex corrections. In (b) $q=t$ for $k=1,\ldots,4$ and $q=b$ for $k=5,6$. In (d) and (e) $q=t$ for $k=1,2$ and $q=b$ for $k=5,6$. In (f), $q=b,t$.

with

$$(G_{lk}^{\tilde{\alpha}})_{ij} = [R^{\tilde{\alpha}} \hat{G}_{lk}^{\tilde{\alpha}} (R^{\tilde{\beta}})^T]_{ij} \quad (l,k=1,\ldots,6), \tag{7}$$

$$(G_k^{\tilde{\alpha}})_{ij} = [R^{\tilde{\alpha}} \hat{G}_k^{\tilde{\alpha}} (R^{\tilde{\beta}})^T]_{ij} \quad (k=1,\ldots,6), \tag{8}$$

where $\hat{G}_k^{\tilde{\alpha}}$ and $\hat{G}_{lk}^{\tilde{\alpha}}$ are the couplings in the $(\tilde{q}_L, \tilde{q}_R)$ basis, and their explicit forms are shown in Appendix A. The notation a_k^α, b_k^α $(k=1,\ldots,6)$, $a_{ik}^{\tilde{q}}, b_{ik}^{\tilde{q}}$ $(k=1,\ldots,4)$, and $l_{ik}^{\tilde{q}}, k_{ik}^{\tilde{q}}$ $(k=1,2)$ used in Eq. (6) is also defined in Appendix A.

The tree-level amplitudes of the three decay processes, as shown in Fig. 1(a), are given by

$$M_1^{(0)} = i \left[R^{\tilde{t}} \begin{pmatrix} -\sqrt{2} m_t h_t \cos\alpha + \dfrac{g m_z \sin(\alpha+\beta)}{c_W} C_{tL} & \dfrac{-h_t}{\sqrt{2}} (A_t \cos\alpha + \mu \sin\alpha) \\ \dfrac{-h_t}{\sqrt{2}} (A_t \cos\alpha + \mu \sin\alpha) & -\sqrt{2} m_t h_t \cos\alpha + \dfrac{g m_z \sin(\alpha+\beta)}{c_W} C_{tR} \end{pmatrix} (R^{\tilde{t}})^T \right]_{21} \tag{9}$$

for $\tilde{t}_2 \to \tilde{t}_1 h^0$,

$$M_2^{(0)} = i \left[R^{\tilde{t}} \begin{pmatrix} -\sqrt{2} m_t h_t \sin\alpha - \dfrac{g m_z \cos(\alpha+\beta)}{c_W} C_{tL} & \dfrac{-h_t}{\sqrt{2}} (A_t \sin\alpha - \mu \cos\alpha) \\ \dfrac{-h_t}{\sqrt{2}} (A_t \sin\alpha - \mu \cos\alpha) & -\sqrt{2} m_t h_t \sin\alpha - \dfrac{g m_z \cos(\alpha+\beta)}{c_W} C_{tR} \end{pmatrix} (R^{\tilde{t}})^T \right]_{21} \tag{10}$$

for $\tilde{t}_2 \to \tilde{t}_1 H^0$, and

$$M_3^{(0)} = \frac{g m_t}{2 m_W} \left[R^{\tilde{t}} \begin{pmatrix} 0 & A_t \cot\beta + \mu \\ -A_t \cot\beta - \mu & 0 \end{pmatrix} (R^{\tilde{t}})^T \right]_{21} \tag{11}$$

for $\tilde{t}_2 \to \tilde{t}_1 A^0$. Here $h_t = g m_t / \sqrt{2} m_W \sin\beta$, $h_b = g m_b / \sqrt{2} m_W \cos\beta$, $C_{tL} = I_{3L}^t - e_t s_W^2$, $C_{tR} = e_t s_w^2$, $s_W = \sin\theta_w$, and $c_w = \cos\theta_w$. $I_{3L}^t = \frac{1}{2}$ and $e_t = \frac{2}{3}$ for the top squark; $I_{3L}^b = -\frac{1}{2}$ and $e_b = -\frac{1}{3}$ for the bottom squark. The tree-level decay width is thus given by

$$\Gamma_s^{(0)} = \frac{|M_s^{(0)}|^2 \lambda^{1/2}(m_{\tilde{t}_2}^2, m_{\tilde{t}_1}^2, m_{H_s^0}^2)}{16\pi m_{\tilde{t}_2}^3}, \tag{12}$$

where $\lambda(x,y,z) = (x-y-z)^2 - 4yz$ and $s = (1,2,3)$ corresponds to the decay into (h^0, H^0, A^0), respectively.

III. YUKAWA CORRECTIONS

The Feynman diagrams contributing to the Yukawa corrections to $\tilde{t}_2 \to \tilde{t}_1 H_i^0$ are shown in Figs. 1(b)–1(f) and Fig. 2. We carried out the calculation in the t'Hooft-Feynman gauge and used dimensional reduction, which preserves supersymmetry, for regularization of the ultraviolet divergences in the virtual loop corrections using the on-mass-shell renormalization scheme [17], in which the fine-structure constant α_{ew} and physical masses are chosen to be the renormalized parameters, and finite parts of the counterterms are fixed by the renormalization conditions. The coupling constant g is related to the input parameters e, m_W, and m_Z via $g^2 = e^2/s_w^2$ and $s_w^2 = 1 - m_W^2/m_Z^2$. As for the renormalization of the parameters in the Higgs sector and the squark sector, it will be described in detail below.

The relevant renormalization constants are defined as

$$m_{W0}^2 = m_W^2 + \delta m_W^2, \quad m_{Z0}^2 = m_Z^2 + \delta m_Z^2,$$

$$m_{q0} = m_q + \delta m_q, \quad m_{\tilde{q}_i 0}^2 = m_{\tilde{q}_i}^2 + \delta m_{\tilde{q}_i}^2,$$

$$A_{q0} = A_q + \delta A_q, \quad \mu_0 = \mu + \delta\mu,$$

$$\theta_{\tilde{q}0} = \theta_{\tilde{q}} + \delta\theta_{\tilde{q}}, \quad \tan\beta_0 = (1 + \delta Z_\beta)\tan\beta,$$

$$\sin\alpha_0 = (1 + \delta Z_\alpha)\sin\alpha,$$

$$\tilde{q}_{i0} = (1 + \delta Z_i^{\tilde{q}})^{1/2} + \delta Z_{ij}^{\tilde{q}} \tilde{q}_j,$$

$$H_0^0 = (1 + \delta Z_{H^0})^{1/2} H^0 + \delta Z_{H^0 h^0} h^0,$$

$$h_0^0 = (1 + \delta Z_{h^0})^{1/2} h^0 + \delta Z_{h^0 H^0} H^0,$$

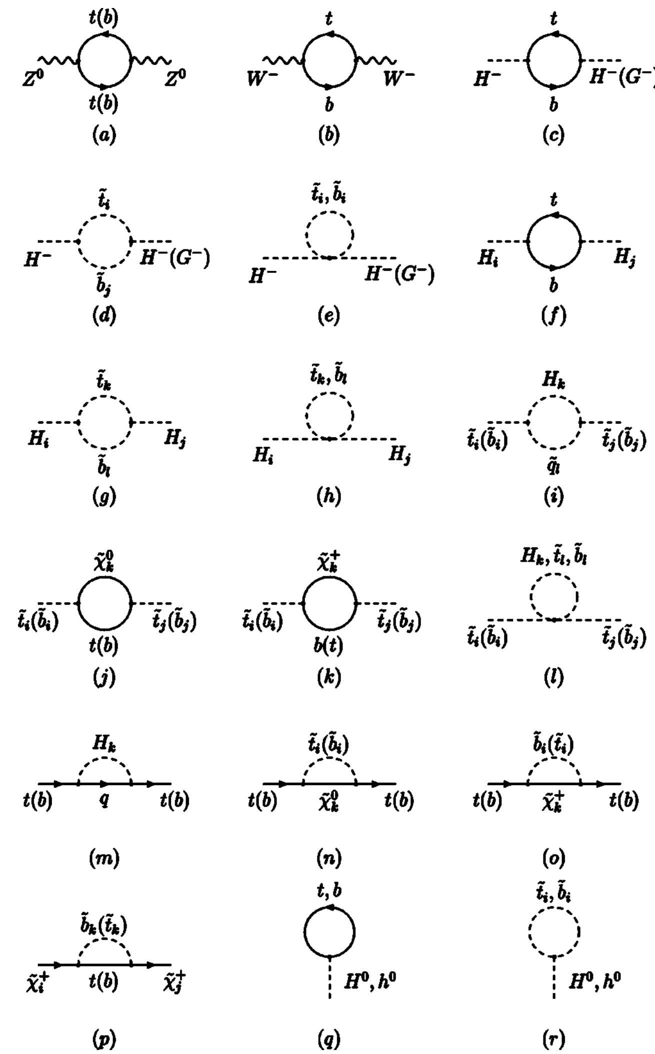

FIG. 2. Feynman diagrams contributing to renormalization constants. In (i) $q = t(b)$ for $k = 1, \ldots, 4$ and $q = b(t)$ for $k = 5,6$. In (f)–(h) $i = j = 1,2,3$ or $i = 1, j = 2$.

$$G_0^- = (1 + \delta Z_{G^-})^{1/2} G^- + \delta Z_{GH} H^-,$$

$$A_0^0 = (1 + \delta Z_{A^0})^{1/2} A^0 \tag{13}$$

with $q = t, b$. Here we introduce the mixing of H^- and G^- [18].

Taking into account the Yukawa corrections, the renormalized amplitude for $\tilde{t}_2 \to \tilde{t}_1 H_s^0$ is given by

$$M_s^{ren} = M_s^{(0)} + \delta M_s^{(v)} + \delta M_s^{(c)}, \tag{14}$$

where $\delta M_s^{(v)}$ and $\delta M_s^{(c)}$ are the vertex corrections and the counterterms, respectively.

The calculations of the vertex corrections from Figs. 1(b)–1(f) result in

$$\delta M^{(v)}_{s=1,2,3}=\frac{i}{16\pi^2}\sum_{k=1}^{6}\sum_{j}(G^{\tilde t}_{sk})_{2j}(G^{\tilde q}_{k})_{j1}B_0(m^2_{\tilde t_1},m_{H^0_k},m_{\tilde q_j})-\frac{i}{16\pi^2}\sum_{k=1}^{6}\sum_{ij}(G^{\tilde t}_{s})_{ij}(G^{\tilde t}_{k})_{2i}(G^{\tilde q}_{k})_{j1}C_0(p_{\tilde t_1},p_{H^0_s},m_{H^0_k},m_{\tilde q_j},m_{\tilde q_i})$$
$$+\frac{i}{16\pi^2}\sum_{k=1}^{6}\sum_{j}(G^{\tilde t}_{sk})_{j1}(G^{\tilde q}_{k})_{2j}B_0(m^2_{\tilde t_2},m_{H^0_k},m_{\tilde q_j})-\frac{i}{16\pi^2}\sum_{ij}\sin\theta_{\tilde t}\cos\theta_{\tilde t}(h_t^2R^{\tilde b}_{i1}R^{\tilde b}_{j1}-h_b^2R^{\tilde b}_{i2}R^{\tilde b}_{j2})$$
$$\times(G^{\tilde b}_{s})_{ij}B_0(m^2_{H^0_s},m_{\tilde b_j},m_{\tilde b_i})-\frac{ih_t^2}{16\pi^2}\{[3(\sin^4\theta_{\tilde t}+\cos^4\theta_{\tilde t})-2\sin^2\theta_{\tilde t}\cos^2\theta_{\tilde t}](G^{\tilde t}_{s})_{21}B_0(m^2_{H^0_s},m_{\tilde t_1},m_{\tilde t_2})$$
$$-8\sin^2\theta_{\tilde t}\cos^2\theta_{\tilde t}(G^{\tilde t}_{s})_{12}B_0(m^2_{H^0_s},m_{\tilde t_2},m_{\tilde t_1})+4\sin\theta_{\tilde t}\cos\theta_{\tilde t}\cos 2\theta_{\tilde t}(G^{\tilde t}_{s})_{11}B_0(m^2_{H^0_s},m_{\tilde t_1},m_{\tilde t_1})$$
$$-4\sin\theta_{\tilde t}\cos\theta_{\tilde t}\cos 2\theta_{\tilde t}(G^{\tilde t}_{s})_{22}B_0(m^2_{H^0_s},m_{\tilde t_2},m_{\tilde t_2})\}+F_{\chi s}, \tag{15}$$

where $F_{\chi s}$ are the remaining terms, which are given by

$$F_{\chi s}=-\frac{ig^2h_t\cos[\alpha-(s-1)\pi/2]}{16\sqrt{2}\pi^2}\sum_i\{[2(a^{\tilde t}_{2i}a^{\tilde t}_{1i}{}^*+b^{\tilde t}_{2i}b^{\tilde t}_{1i}{}^*)m_t][(2m^2_{\tilde t_1}+p_{\tilde t_1}p_{H^0_s})C_{11}$$
$$+(2p_{\tilde t_1}p_{H^0_s}+m^2_{H^0_s})C_{12}+2m^2_{\tilde t_1}C_{21}+2m^2_{H^0_s}C_{22}+4p_{\tilde t_1}p_{H^0_s}C_{23}+8C_{24}]$$
$$+[2(a^{\tilde t}_{2i}b^{\tilde t}_{1i}{}^*+b^{\tilde t}_{2i}a^{\tilde t}_{1i}{}^*)m_{\tilde\chi^0_i}][(2m^2_{\tilde t_1}+p_{\tilde t_1}p_{H^0_s})C_{11}+(2p_{\tilde t_1}p_{H^0_s}+m^2_{H^0_s})C_{12}+(m^2_{\tilde t_1}C_{21}+m^2_{H^0_s}C_{22}+2p_{\tilde t_1}p_{H^0_s}C_{23}+4C_{24}$$
$$+(m^2_{\tilde t_1}+p_{\tilde t_1}p_{H^0_s})C_0+m_t^2C_0]\}(p_{\tilde t_1},p_{H^0_s},m_{\tilde\chi^0_i},m_t,m_t)+\frac{ig^2h_b\sin[\alpha-(s-1)\pi/2]}{16\sqrt{2}\pi^2}$$
$$\times\sum_i\{[2(l^{\tilde t}_{2i}l^{\tilde t}_{1i}{}^*+k^{\tilde t}_{2i}k^{\tilde t}_{1i}{}^*)m_b][(2m^2_{\tilde t_1}+p_{\tilde t_1}p_{H^0_s})C_{11}+(2p_{\tilde t_1}p_{H^0_s}+m^2_{H^0_s})C_{12}+2m^2_{\tilde t_1}C_{21}$$
$$+2m^2_{H^0_s}C_{22}+4p_{\tilde t_1}p_{H^0_s}C_{23}+8C_{24}]+[2(l^{\tilde t}_{2i}k^{\tilde t}_{1i}{}^*+k^{\tilde t}_{2i}l^{\tilde t}_{1i}{}^*)m_{\tilde\chi^-_i}][(2m^2_{\tilde t_1}+p_{\tilde t_1}p_{H^0_s})C_{11}+(2p_{\tilde t_1}p_{H^0_s}+m^2_{H^0_s})C_{12}$$
$$+(m^2_{\tilde t_1}C_{21}+m^2_{H^0_s}C_{22}+2p_{\tilde t_1}p_{H^0_s}C_{23}+4C_{24}+(m^2_{\tilde t_1}+p_{\tilde t_1}p_{H^0_s})C_0+m_b^2C_0]\}(p_{\tilde t_1},p_{H^0_s},m_{\tilde\chi^-_i},m_b,m_b) \tag{16}$$

for $s=(1,2)$, and

$$F_{\chi 3}=-\frac{g^3m_t\cot\beta}{32\pi^2m_W}\sum_i\{[2(a^{\tilde t}_{2i}a^{\tilde t}_{1i}{}^*-b^{\tilde t}_{2i}b^{\tilde t}_{1i}{}^*)m_t](m^2_{A^0}C_{12}+p_{\tilde t_1}p_{A^0}C_{11})$$
$$+[2(a^{\tilde t}_{2i}b^{\tilde t}_{1i}{}^*-b^{\tilde t}_{2i}a^{\tilde t}_{1i}{}^*)m_{\tilde\chi^0_i}][(2m^2_{\tilde t_1}+p_{\tilde t_1}p_{A^0})C_{11}+(2p_{\tilde t_1}p_{A^0}+m^2_{A^0})C_{12}$$
$$+m^2_{\tilde t_1}C_{21}+m^2_{A^0}C_{22}+2p_{\tilde t_1}p_{A^0}C_{23}+4C_{24}+(p^2_{\tilde t_1}+p_{\tilde t_1}p_{A^0})C_0-m_t^2C_0]\}(p_{\tilde t_1},p_{A^0},m_{\tilde\chi^0_i},m_t,m_t)$$
$$-\frac{ig^3m_b\tan\beta}{32\pi^2m_W}\sum_i\{[2(l^{\tilde t}_{2i}l^{\tilde t}_{1i}{}^*-k^{\tilde t}_{2i}k^{\tilde t}_{1i}{}^*)m_b](m^2_{A^0}C_{12}+p_{\tilde t_1}p_{A^0}C_{11})$$
$$+[2(l^{\tilde t}_{2i}k^{\tilde t}_{1i}{}^*-k^{\tilde t}_{2i}l^{\tilde t}_{1i}{}^*)m_{\tilde\chi^-_i}][(2m^2_{\tilde t_1}+p_{\tilde t_1}p_{A^0})C_{11}+(2p_{\tilde t_1}p_{A^0}+m^2_{A^0})C_{12}$$
$$+m^2_{\tilde t_1}C_{21}+m^2_{A^0}C_{22}+2p_{\tilde t_1}p_{A^0}C_{23}+4C_{24}+(p^2_{\tilde t_1}+p_{\tilde t_1}p_{A^0})C_0-m_b^2C_0]\}(p_{\tilde t_1},p_{A^0},m_{\tilde\chi^-_i},m_b,m_b) \tag{17}$$

for $s=3$. In the above expressions, B_0 and $C_{i(j)}$ are as defined by Passarino and Veltman [20], except we work in the metric $(1,-1,-1,-1)$. For $q=t$, we have $k=1,\ldots,4$. For $q=b$, we have $k=5,6$.

The counterterms can be expressed as

$$\delta M_1^{(c)}=i(G_1^{\tilde t})_{21}\left[\frac{1}{2}(\delta Z_1+\delta Z_2+\delta Z_{h^0})-2\tan 2\theta_{\tilde t}\delta\theta_{\tilde t}+\frac{\delta g}{g}-\frac{\delta m_W^2}{2m_W^2}-\cos^2\beta\,\delta\beta\right]$$
$$-i\frac{gm_tA_t\cos\alpha}{2m_W\sin\beta}\cos 2\theta_{\tilde t}\left[\frac{A_t\delta m_t+m_t\delta A_t}{m_tA_t}+\tan^2\alpha\,\delta Z_\alpha\right]-i\frac{gm_t\mu\sin\alpha}{2m_W\sin\beta}\cos 2\theta_{\tilde t}\left[\frac{\delta\mu}{\mu}+\frac{\delta m_t}{m_t}-\delta Z_\alpha\right]$$
$$+i(G_1^{\tilde t})_{11}\delta Z_{12}+i(G_1^{\tilde t})_{22}\delta Z_{21}+i(G_2^{\tilde t})_{21}\delta Z_{H^0h^0}, \tag{18}$$

$$\delta M_2^{(c)}=i(G_2^{\tilde t})_{21}\left[\frac{1}{2}(\delta Z_1+\delta Z_2+\delta Z_{H^0})-2\tan 2\theta_{\tilde t}\delta\theta_{\tilde t}+\frac{\delta g}{g}-\frac{\delta m_W^2}{2m_W^2}-\cos^2\beta\,\delta\beta\right]$$
$$-i\frac{gm_tA_t\sin\alpha}{2m_W\sin\beta}\cos 2\theta_{\tilde t}\left[\frac{A_t\delta m_t+m_t\delta A_t}{m_tA_t}+\delta Z_\alpha\right]+i\frac{g\mu m_t\cos\alpha}{2m_W\sin\beta}\cos 2\theta_{\tilde t}\left[\frac{\delta\mu}{\mu}+\frac{\delta m_t}{m_t}-\tan^2\alpha\,\delta Z_\alpha\right]$$
$$+i(G_2^{\tilde t})_{11}\delta Z_{12}+i(G_2^{\tilde t})_{22}\delta Z_{21}+i(G_1^{\tilde t})_{21}\delta Z_{h^0H^0}, \tag{19}$$

$$\delta M_3^{(c)}=i(G_3^{\tilde t})_{21}\left[\frac{1}{2}(\delta Z_1+\delta Z_2+\delta Z_{A^0})+\frac{\delta g}{g}-\frac{\delta m_W^2}{2m_W^2}\right]-\frac{gm_tA_t\cos\alpha}{2m_W}\cot\beta\left[\frac{\delta(m_tA_t)}{m_tA_t}-\delta Z_\beta\right]-\frac{g\mu m_t}{2m_W}\left[\frac{\delta\mu}{\mu}+\frac{\delta m_t}{m_t}\right]. \tag{20}$$

Here we consider only the counterterms from the Yukawa couplings, and the explicit expressions for some renormalization constants calculated from the self-energy diagrams in Fig. 2 are given in Appendix B. Other renormalization constants are fixed as follows.

For δZ_{GH}, using the approach discussed in the two-Higgs doublet model in [18], we derived below its expression in the MSSM, where the version of the Higgs potential is different from that of Ref. [18]. First, the one-loop renormalized two-point function is given by

$$i\Gamma_{GH}(p^2)=i(p^2-m_{H^-}^2)\delta Z_{HG}+ip^2\delta Z_{GH}-iT_{GH}+i\Sigma_{GH}(p^2), \tag{21}$$

where T_{GH} is the tadpole function, which is given by

$$T_{GH}=\frac{g}{2m_W}[T_{H_2}\sin(\alpha-\beta)+T_{H_1}\cos(\alpha-\beta)]. \tag{22}$$

Next, from the on-shell renormalization condition, we obtained

$$\delta Z_{GH}=\frac{1}{m_{H^-}^2}[T_{GH}-\Sigma_{GH}(m_{H^-}^2)]. \tag{23}$$

The explicit expressions of Σ_{GH} and the tadpole counterterms T_{H_k} $(k=1,2)$ are given in Appendix B.

For the renormalization of the parameter β, following the analysis of Ref. [19], we fixed the renormalization constant by the requirement that the on-mass-shell $H^+\overline{\tau}\nu_\tau$ coupling retains the same form as in Eq. (3) of Ref. [19] to all orders of perturbation theory. However, by introducing the mixing of H^- and G^- instead of H^- and W^-, the expression for δZ_β is then changed to

$$\delta Z_\beta=\frac{1}{2}\frac{\delta m_W^2}{m_W^2}-\frac{1}{2}\frac{\delta m_Z^2}{m_Z^2}+\frac{1}{2}\frac{\delta m_Z^2-\delta m_W^2}{m_Z^2-m_W^2}-\frac{1}{2}\delta Z_{H^+}+\cot\beta\,\delta Z_{GH}. \tag{24}$$

For the counterterm of the squark mixing angle $\theta_{\tilde q}$, using the same renormalized scheme as Ref. [10], one has

$$\delta\theta_{\tilde q}=\frac{\mathrm{Re}[\Sigma_{12}^{\tilde q}(m_{\tilde q_1}^2)+\Sigma_{12}^{\tilde q}(m_{\tilde q_2}^2)]}{2(m_{\tilde q_1}^2-m_{\tilde q_2}^2)}, \tag{25}$$

where the explicit expressions for the Σ_{ij} functions arising from the self-energy diagrams due to the Yukawa couplings are given in Appendix B.

For the renormalization of the soft SUSY-breaking parameter A_q, we fixed its counterterm by keeping the tree-level relation of A_q, $m_{\tilde q_i}$, and $\theta_{\tilde q}$ [21], and got the following expression:

$$\delta A_q=\frac{m_{\tilde q_1}^2-m_{\tilde q_2}^2}{2m_q}\left(2\cos 2\theta_{\tilde q}\delta\theta_{\tilde q}-\sin 2\theta_{\tilde q}\frac{\delta m_q}{m_q}\right)+\frac{\sin 2\theta_{\tilde q}}{2m_q}(\delta m_{\tilde q_1}^2-\delta m_{\tilde q_2}^2)+\{\cot\beta,\tan\beta\}\delta\mu+\delta\{\cot\beta,\tan\beta\}\mu. \tag{26}$$

As for the parameter μ, there are several schemes [11,22,23] to fix its counterterm, and here we use the on-shell renormalization scheme in Ref. [23], which gives

$$\delta\mu=\sum_{k=1}^{2}\left[m_{\tilde{\chi}_k^+}(\delta U_{k2}V_{k2}+U_{k2}\delta V_{k2})+\delta m_{\tilde{\chi}_k^+}U_{k2}V_{k2}\right], \tag{27}$$

where (U,V) are the two 2×2 matrices diagonalizing the chargino mass matrix, and their counterterms $(\delta U,\delta V)$ are given by

$$\delta U=\frac{1}{4}(\delta Z_R-\delta Z_R^T)U, \tag{28}$$

$$\delta V=\frac{1}{4}(\delta Z_L-\delta Z_L^T)V. \tag{29}$$

The mass shifts $\delta m_{\tilde{\chi}_k^+}$ and the off-diagonal wave function renormalization constants $\delta Z_{R(L)}$ can be written as

$$\delta m_{\tilde{\chi}_k^+}=\frac{1}{2}\mathrm{Re}\{m_{\tilde{\chi}_k^+}[\Pi_{kk}^L(m_{\tilde{\chi}_k^+}^2)+\Pi_{kk}^R(m_{\tilde{\chi}_k^+}^2)]+\Pi_{kk}^{S,L}(m_{\tilde{\chi}_k^+}^2)+\Pi_{kk}^{S,R}(m_{\tilde{\chi}_k^+}^2)\}, \tag{30}$$

$$(\delta Z_R)_{ij}=\frac{2}{m_{\tilde{\chi}_i^+}^2-m_{\tilde{\chi}_j^+}^2}\mathrm{Re}[\Pi_{ij}^R(m_{\tilde{\chi}_j^+}^2)m_{\tilde{\chi}_j^+}^2+\Pi_{ij}^L(m_{\tilde{\chi}_j^+}^2)m_{\tilde{\chi}_i^+}m_{\tilde{\chi}_j^+}+\Pi_{ij}^{S,R}(m_{\tilde{\chi}_j^+}^2)m_{\tilde{\chi}_i^+}+\Pi_{ij}^{S,L}(m_{\tilde{\chi}_j^+}^2)m_{\tilde{\chi}_j^+}], \tag{31}$$

$$(\delta Z_L)_{ij}=(\delta Z_R)_{ij}\quad (L\leftrightarrow R). \tag{32}$$

The explicit expressions of the chargino self-energy matrices $\Pi^{L(R)}$ and $\Pi^{S,L(R)}$ are given in Appendix B.

Finally, the renormalized decay width is then given by

$$\Gamma_s=\Gamma_s^{(0)}+\delta\Gamma_s^{(v)}+\delta\Gamma_s^{(c)} \tag{33}$$

with

$$\delta\Gamma_s^{(a)}=\frac{\lambda^{1/2}(m_{\tilde{t}_2}^2,m_{\tilde{t}_1}^2,m_{H_s^0}^2)}{8\pi m_{\tilde{t}_2}^3}\mathrm{Re}\{M_s^{(0)*}\delta M_s^{(a)}\}\quad (a=v,c). \tag{34}$$

IV. NUMERICAL RESULTS AND CONCLUSION

We now present some numerical results for the Yukawa corrections to the decays $\tilde{t}_2\to\tilde{t}_1+(h^0,H^0,A^0)$. The SM input parameters in our calculations were taken to be $\alpha_{ew}(m_Z)=1/128.8$, $m_W=80.375$ GeV, $m_Z=91.1867$ GeV [24], $m_t=175.6$ GeV, and $m_b=4.25$ GeV.

In order to improve the convergence of the perturbation expansion, using the method presented in Ref. [16], we take into account the QCD and SUSY QCD running quark masses $\hat{m}_q(Q)[\hat{m}_t(Q),\hat{m}_b(Q)]$ and running trilinear coupling $\hat{A}_t$ in our calculation (the energy scale Q here is the mass of the heavier top squark, i.e., $m_{\tilde{t}_2}$). In the tree-level $H_s^0\tilde{t}_2\tilde{t}_1$ couplings, we use $\hat{m}_t(Q)$ and $\hat{A}_t$ instead of the on-shell parameters, while in the calculation of the one-loop corrections, all parameters are on shell except the Yukawa couplings h_t,h_b taken as the running quark masses.

$\hat{m}_q(Q)$ are evaluated by the next-to-leading order formula [25,26]

$$\hat{m}_b(Q)=U_6(Q,m_t)U_5(m_t,m_b)m_b(m_b),$$

$$\hat{m}_t(Q)=U_6(Q,m_t)m_t(m_t), \tag{35}$$

where we have assumed that there are no other colored particles with masses between the scale Q and m_t, and $\hat{m}_b(m_b)=4.25$ GeV, $\hat{m}_t(m_t)=175.6$ GeV [27]. The evolution factor U_f is

$$U_f(Q_2,Q_1)=\left(\frac{\alpha_s(Q_2)}{\alpha_s(Q_1)}\right)^{d^{(f)}}\left[1+\frac{\alpha_s(Q_1)-\alpha_s(Q_2)}{4\pi}J^{(f)}\right],$$

$$d^{(f)}=\frac{12}{33-2f},\qquad J^{(f)}=-\frac{8982-504f+40f^2}{3(33-2f)^2}, \tag{36}$$

where $\alpha_s(Q)$ is given by the solutions of the two-loop renormalization group equations [28]. When $Q=400$ GeV, the running mass $\hat{m}_b(Q)\sim 2.5$ GeV. In addition, we also improved the perturbation calculations by the following replacement [25,26]:

$$\hat{m}_t(Q)\to\frac{\hat{m}_t(Q)}{1+\Delta m_t(M_{SUSY\ QCD})}, \tag{37}$$

$$\hat{m}_b(Q)\to\frac{\hat{m}_b(Q)}{1+\Delta m_b(M_{SUSY})}, \tag{38}$$

where

$$\Delta m_t=-\frac{\alpha_s}{3\pi}\left\{\overline{B}_1(0,m_{\tilde{g}},m_{\tilde{t}_1})+\overline{B}_1(0,m_{\tilde{g}},m_{\tilde{t}_2})-\sin 2\theta_t\left(\frac{m_{\tilde{g}}}{m_t}\right)\times[\overline{B}_0(0,m_{\tilde{g}},m_{\tilde{t}_1})-\overline{B}_0(0,m_{\tilde{g}},m_{\tilde{t}_2})]\right\}, \tag{39}$$

$$\Delta m_b=\frac{2\alpha_s}{3\pi}M_{\tilde{g}}\mu\tan\beta I(m_{\tilde{b}_1},m_{\tilde{b}_2},M_{\tilde{g}})+\frac{h_t^2}{16\pi^2}\mu A_t\tan\beta I(m_{\tilde{t}_1},m_{\tilde{t}_2},\mu)-\frac{g^2}{16\pi^2}\mu M_2\tan\beta\left[\cos^2\theta_{\tilde{t}}I(m_{\tilde{t}_1},M_2,\mu)+\sin^2\theta_{\tilde{t}}I(m_{\tilde{t}_2},M_2,\mu)+\frac{1}{2}\cos^2\theta_{\tilde{b}}I(m_{\tilde{b}_1},M_2,\mu)+\frac{1}{2}\sin^2\theta_{\tilde{b}}I(m_{\tilde{b}_2},M_2,\mu)\right] \tag{40}$$

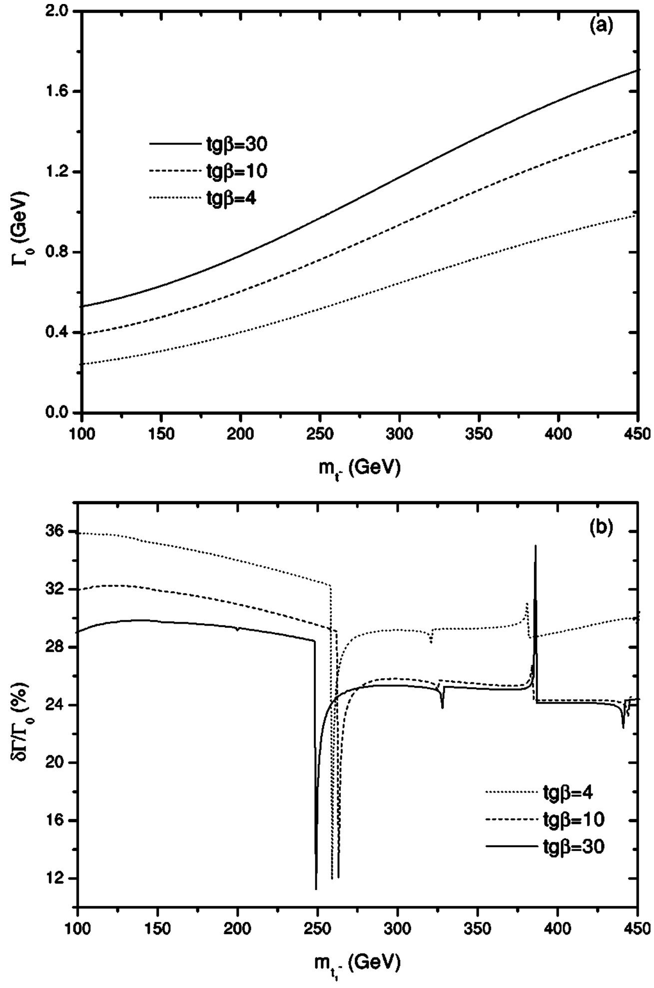

FIG. 3. The tree-level decay width (a) of $\tilde{t}_2 \to \tilde{t}_1 h^0$ and its Yukawa corrections (b) as functions of $m_{\tilde{t}_1}$ for $\tan\beta = 4$, 10, and 30, respectively, assuming $m_{A^0} = 150$ GeV, $\mu = M_2 = 200$ GeV, $A_t = A_b = 600$ GeV, and $M_{\tilde{Q}} = 1.5 M_{\tilde{U}} = 1.5 M_{\tilde{D}}$.

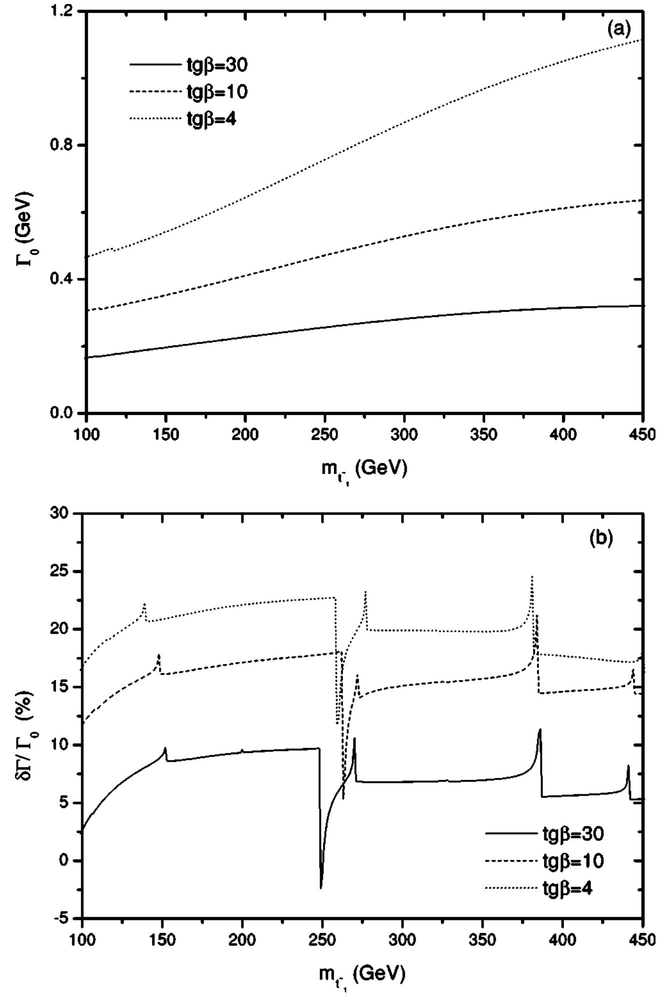

FIG. 4. The tree-level decay width (a) of $\tilde{t}_2 \to \tilde{t}_1 H^0$ and its Yukawa corrections (b) as functions of $m_{\tilde{t}_1}$ for $\tan\beta = 4$, 10, and 30, respectively, assuming $m_{A^0} = 150$ GeV, $\mu = M_2 = 200$ GeV, $A_t = A_b = 600$ GeV, and $M_{\tilde{Q}} = 1.5 M_{\tilde{U}} = 1.5 M_{\tilde{D}}$.

with $\overline{B_1} = B_1 + \Delta/2$, $\overline{B_0} = B_0 - \Delta$ $(\Delta = 1/\epsilon - \gamma_E + \ln 4\pi)$, and

$$I(a,b,c) = \frac{1}{(a^2-b^2)(b^2-c^2)(a^2-c^2)}\left(a^2 b^2 \log\frac{a^2}{b^2} + b^2 c^2 \log\frac{b^2}{c^2} + c^2 a^2 \log\frac{c^2}{a^2}\right). \tag{41}$$

The running trilinear couplings $\hat{A}_t$ can be obtained according to the definition of the $\overline{DR}$ renormalized quantities [16,30]. First we compute the running top squark masses $\hat{m}^2_{\tilde{t}_i}(Q) = \hat{m}^2_{\tilde{t}_i} + \delta\hat{m}^2_{\tilde{t}_i}$ and the running mixing angle of the top squarks $\hat{\theta}_{\tilde{t}}(Q) = \hat{\theta}_{\tilde{t}} + \delta\hat{\theta}_{\tilde{t}}$, where the counterterms $\delta\hat{m}^2_{\tilde{t}_i}$ and $\delta\hat{\theta}_{\tilde{t}}$ are given by

$$\delta\hat{m}^2_{\tilde{t}_i} = \mathrm{Re}[\Sigma^{\tilde{g}(g)}_{ii}(m^2_{\tilde{t}_i}) + \Sigma^{\tilde{t}(\tilde{g})}_{ii}(m^2_{\tilde{t}_i}) + \Sigma^{\tilde{t}(\tilde{t})}_{ii}],$$

$$\delta\hat{\theta}_{\tilde{t}} = \frac{1}{2}\,\frac{\mathrm{Re}\{\Sigma^{\tilde{t}}_{12}(m^2_{\tilde{t}_1}) + \Sigma^{\tilde{t}}_{12}(m^2_{\tilde{t}_2})\}}{m^2_{\tilde{t}_1} - m^2_{\tilde{t}_2}}. \tag{42}$$

Here the explicit expressions for the Σ_{ij} functions arising from the QCD self-energy diagrams are given in Ref. [26]. Then we can get the running parameter $\hat{A}_t$ from the formula

$$\hat{m}_t \hat{A}_t = [\hat{m}^2_{\tilde{t}_1}(Q) - \hat{m}^2_{\tilde{t}_2}(Q)]\sin\hat{\theta}_{\tilde{t}}(Q)\cos\hat{\theta}_{\tilde{t}}(Q) + \hat{m}_t \mu \cot\beta. \tag{43}$$

The two-loop leading-log relations [29] of the neutral Higgs boson masses and mixing angles in the MSSM were used. For m_{H^+} the tree-level formula was used. Other MSSM parameters were determined as follows.

(i) For the parameters M_1, M_2, and μ in the chargino and neutralino matrix, we take M_2 and μ as the input parameters, and then use the relation $M_1 = (5/3)(g'^2/g^2)M_2 \simeq 0.5 M_2$ [2,31] to determine M_1. The gluino mass $m_{\tilde{g}}$ was related to M_2 by $m_{\tilde{g}} = [\alpha_s(m_{\tilde{g}})/\alpha_2]M_2$ [7].

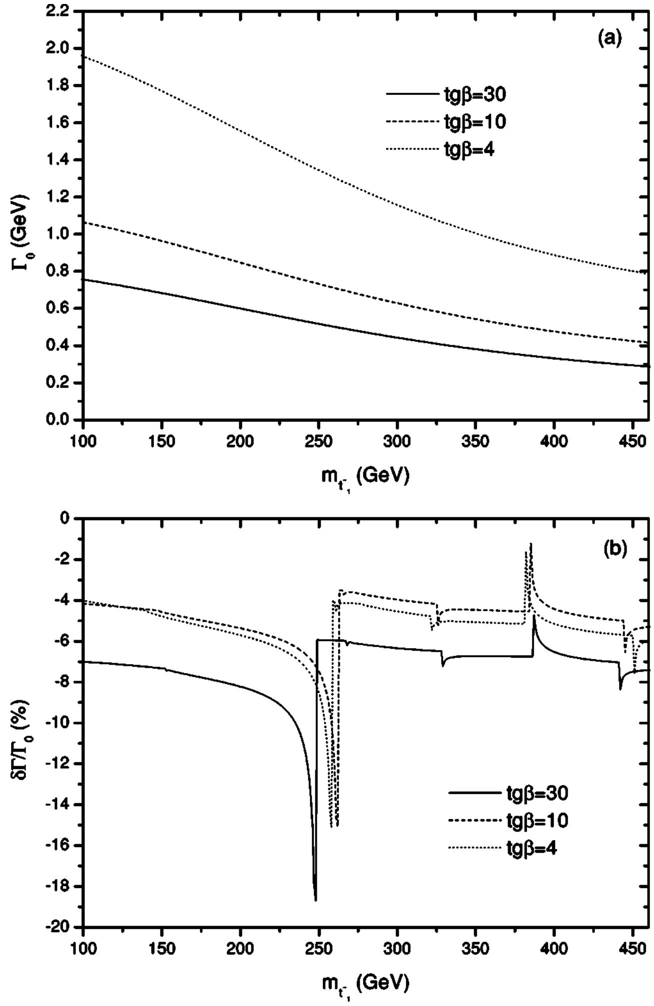

FIG. 5. The tree-level decay width (a) of $\tilde{t}_2 \to \tilde{t}_1 A^0$ and its Yukawa corrections (b) as functions of $m_{\tilde{t}_1}$ for $\tan\beta = 4$, 10, and 30, respectively, assuming $m_{A^0} = 150$ GeV, $\mu = M_2 = 200$ GeV, $A_t = A_b = 600$ GeV, and $M_{\tilde{Q}} = 1.5 M_{\tilde{U}} = 1.5 M_{\tilde{D}}$.

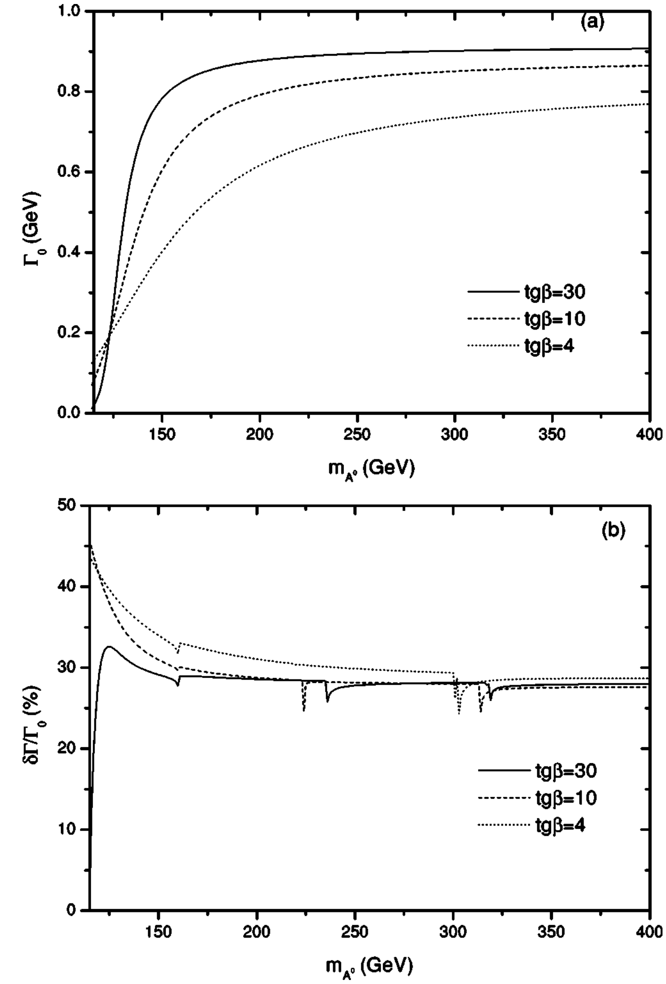

FIG. 6. The tree-level decay width (a) of $\tilde{t}_2 \to \tilde{t}_1 h^0$ and its Yukawa corrections (b) as functions of m_{A^0} for $\tan\beta = 4$, 10, and 30, respectively, assuming $m_{\tilde{t}_1} = 200$ GeV, $\mu = M_2 = 200$ GeV, $A_t = A_b = 600$ GeV, and $M_{\tilde{Q}} = 1.5 M_{\tilde{U}} = 1.5 M_{\tilde{D}}$.

(ii) For the parameters $m^2_{\tilde{Q},\tilde{U},\tilde{D}}$ and $A_{t,b}$ in the squark mass matrices, we assumed $M_{\tilde{Q}} = 1.5 M_{\tilde{U}} = 1.5 M_{\tilde{D}}$ and $A_t = A_b$ to simplify the calculations, except for Figs. 10 and 11, where we assumed $M_{\tilde{D}} = 1.12 M_{\tilde{Q}}$ and $A_t = A_b$ in order to compare with the SUSY QCD results in Ref. [8].

Some typical numerical results for the tree-level decay widths and the Yukawa corrections are given in Figs. 3–12.

Figures 3–5 show the $m_{\tilde{t}_1}$ dependence of the results of the three decay channels. Here we take $m_{A^0} = 150$ GeV, $\mu = M_2 = 200$ GeV, and $A_t = A_b = 600$ GeV. The leading terms of the tree-level amplitudes $M_s^{(0)} (s = 1,2,3)$ are given by

$$M_1^{(0)} = \frac{-ig\hat{m}_t}{2m_W \sin\beta} (\hat{A}_t \cos\alpha + \mu \sin\alpha) \cos 2\theta_{\tilde{t}}, \quad (44)$$

$$M_2^{(0)} = \frac{-ig\hat{m}_t}{2m_W \sin\beta} (\hat{A}_t \sin\alpha - \mu \cos\alpha) \cos 2\theta_{\tilde{t}}, \quad (45)$$

$$M_3^{(0)} = \frac{-g\hat{m}_t}{2m_W} (\hat{A}_t \cot\beta + \mu). \quad (46)$$

For $m_{\tilde{t}_1} = 100$ GeV, $\cos\theta_{\tilde{t}} \sim (-0.575, -0.574, -0.574)$, and $\cos\alpha \sim (0.754, 0.953, 1.000)$ for $\tan\beta = 4$, 10, and 30 , respectively, and for $m_{\tilde{t}_1} = 560$ GeV, $\cos\theta_{\tilde{t}} \sim (-0.323, -0.332, -0.334)$, and $\cos\alpha \sim (0.737, 0.897, 0.992)$ for $\tan\beta \sim 4$, 10, and 30, respectively. In the case of $i = 2$, the two terms in Eq. (45) have opposite signs, and their magnitudes get close to each other with increasing $\tan\beta$ and thus cancel to large extent for large $\tan\beta$. Therefore, the tree-level decay widths have the feature $\Gamma_0(\tan\beta = 4) > \Gamma_0(\tan\beta = 10) > \Gamma_0(\tan\beta = 30)$ in most of the parameter space, as shown in Fig. 4(a). In the case of $i = 1$, the two terms in Eq. (44) have the same signs and there are no canceling effects between them, so Γ_0 is larger than in the case of $i = 2$ for the same values of $\tan\beta$. In the case of $i = 3$, the amplitude contains a term proportional to $\cot\beta$, so $\Gamma_0(\tan\beta = 4) > \Gamma_0(\tan\beta = 10) > \Gamma_0(\tan\beta = 30)$. From Figs. 3–5(b), one can see that the relative corrections are sensitive to the value of $\tan\beta$.

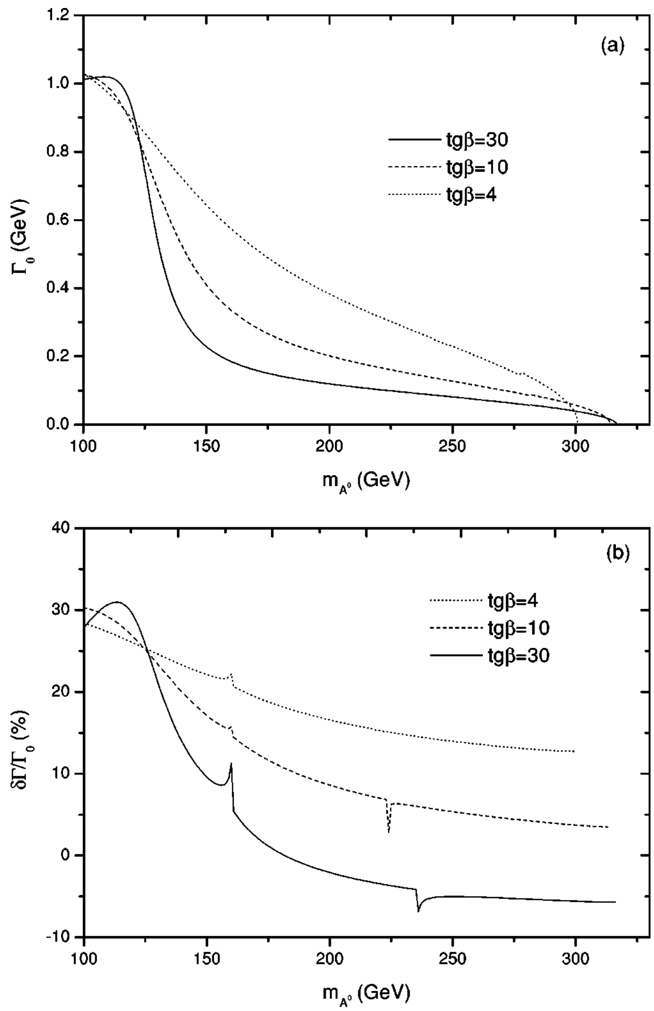

FIG. 7. The tree-level decay width (a) of $\tilde{t}_2 \rightarrow \tilde{t}_1 H^0$ and its Yukawa corrections (b) as functions of m_{A^0} for $\tan\beta=4$, 10, and 30, respectively, assuming $m_{\tilde{t}_1}=200$ GeV, $\mu=M_2=200$ GeV, $A_t=A_b=600$ GeV, and $M_{\tilde{Q}}=1.5M_{\tilde{U}}=1.5M_{\tilde{D}}$.

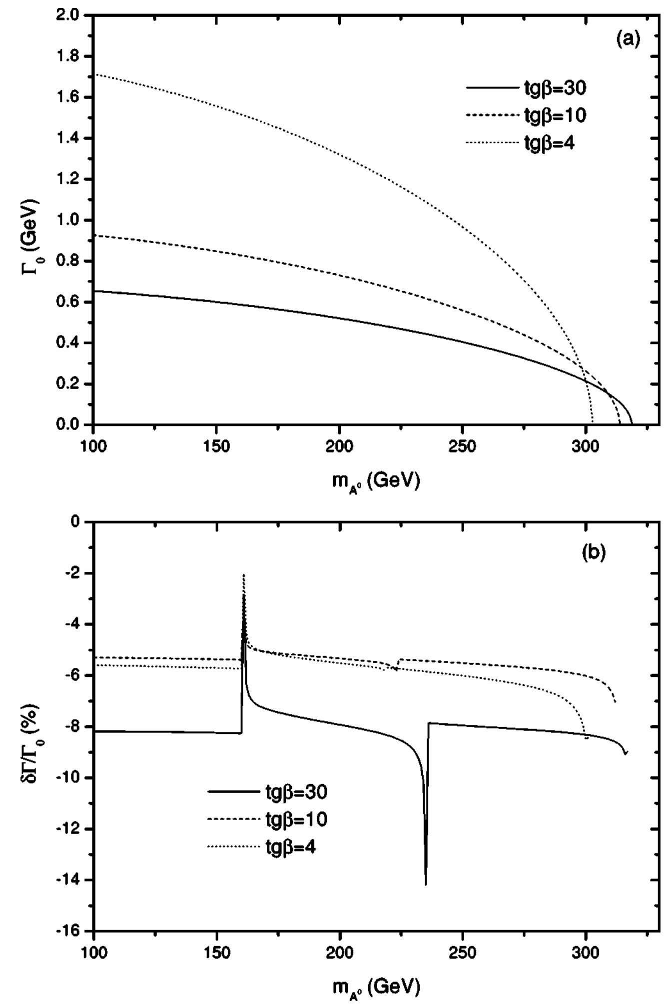

FIG. 8. The tree-level decay width (a) of $\tilde{t}_2 \rightarrow \tilde{t}_1 A^0$ and its Yukawa corrections (b) as functions of m_{A^0} for $\tan\beta=4$, 10, and 30, respectively, assuming $m_{\tilde{t}_1}=200$ GeV, $\mu=M_2=200$ GeV, $A_t=A_b=600$ GeV, and $M_{\tilde{Q}}=1.5M_{\tilde{U}}=1.5M_{\tilde{D}}$.

For $\tan\beta=4$ and 30, the magnitudes of the corrections can exceed 30% and 20%, respectively, for the decay into h^0. For $\tan\beta=10$, the corrections are medium in Fig. 3(b) and Fig. 4(b), and smallest in Fig. 5(b). In general, for low $\tan\beta$ the top quark contribution is enhanced while for high $\tan\beta$ the bottom quark contribution becomes large, and for medium $\tan\beta$, there are no enhanced effects from the Yukawa couplings. There are some dips and peaks in Figs. 3–5(b), which arise from the singularities at the threshold points $m_{\tilde{t}_1}=m_{\tilde{\chi}_i^0}+m_t$ and $m_{\tilde{t}_2}=m_{\tilde{b}_2}+m_{G^+}(=m_W)$, respectively.

Figures 6–8 give the tree-level decay widths and the Yukawa corrections as functions of m_{A^0} for the three decays. We assumed $m_{\tilde{t}_1}=200$ GeV, $\mu=M_2=200$ GeV, and $A_t=A_b=1$ TeV. The features of the tree-level decay widths in Figs. 6(a)–8(a) are similar to Figs. 3(a)–5(a), respectively. From Figs. 6(b)–8(b) we can see that the relative corrections decrease or increase the decay widths depending on $\tan\beta$. In most of the range of mass of A^0, the relative corrections vary from 27% to 33% for the decay into h^0, -6% to 20% for the decay into H^0, and -9% to -5% for the decay into A^0.

There are many dips and peaks on the curves in Figs. 6(b)–8(b), which come from the singularities at the threshold points. For example, at $m_{A^0}=235$ GeV in Fig. 8(b), we have the threshold point $m_{\tilde{b}_1}=m_{\tilde{\chi}_4^0}+m_b$ for $\tan\beta=30$.

In Fig. 9 we present the tree-level decay widths and the Yukawa corrections as the functions of μ in the case of $\tilde{t}_2 \rightarrow \tilde{t}_1+H_i^0$, assuming $\tan\beta=30$, $m_{\tilde{t}_1}=250$ GeV, $M_2=100$ GeV, $A_t=250$ GeV, $A_b=-250$ GeV, and $m_{A^0}=150$ GeV. In most of the parameter μ range, the relative corrections are from 12% to 32% for the decay into h^0, and only a few percent for the decay into A^0 except near the zero point of Γ_0. For the decay into H^0, when μ takes certain values (near -26 GeV), Γ_0 gets very small ($\lesssim 10^{-4}$ GeV), and the relative corrections near these values do not have a physical meaning. So we cut off the corrections, since perturbation theory breaks down here. In order to improve the results, we use the running Higgsino mass parameter $\hat{\mu}(Q)=\mu+\delta\hat{\mu}(Q)$ in the tree-level coupling, and find that the convergence of the perturbation expansion becomes better as shown by the dashed line in Fig. 9(b), where

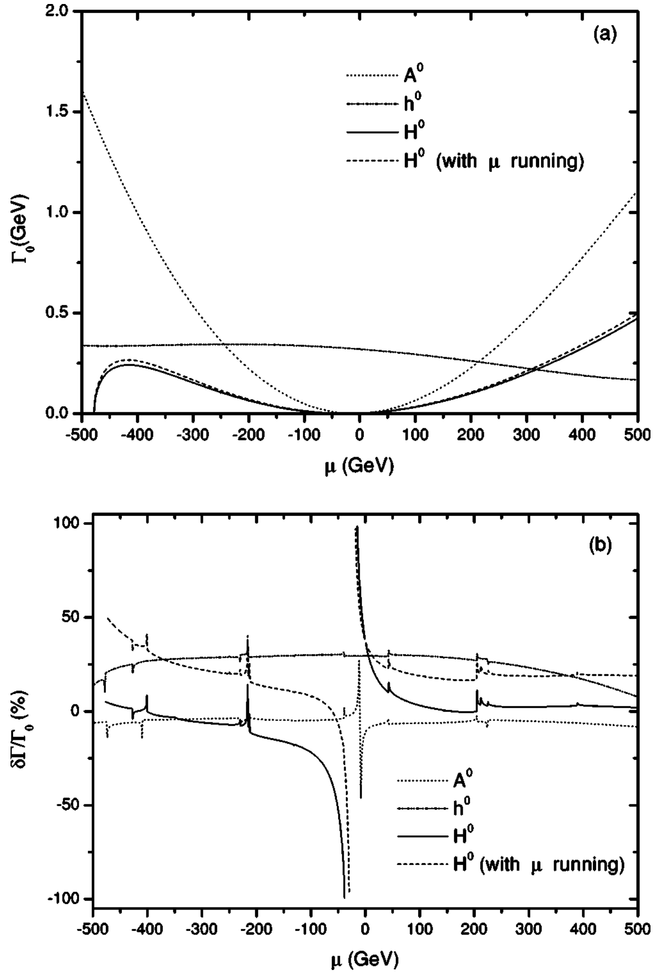

FIG. 9. The tree-level decay width (a) of $\tilde{t}_2 \to \tilde{t}_1 H_i^0$ and its Yukawa corrections (b) as functions of μ, assuming $\tan\beta = 30$, $m_{\tilde{t}_1} = 250$ GeV, $M_2 = 100$ GeV, $A_t = 250$ GeV, $A_b = -250$ GeV, $m_{A^0} = 150$ GeV, and $M_{\tilde{Q}} = 1.5 M_{\tilde{U}} = 1.5 M_{\tilde{D}}$.

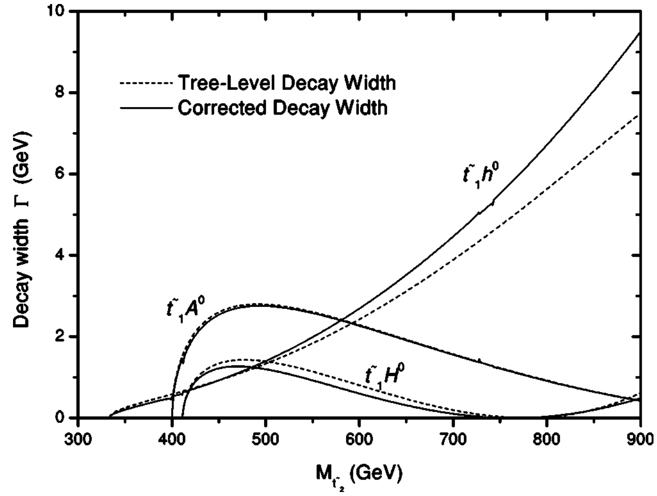

FIG. 10. The decay width of $\tilde{t}_2 \to \tilde{t}_1 H_i^0$ as a function of $m_{\tilde{t}_2}$, assuming $\tan\beta = 3$, $\cos\theta_{\tilde{t}} = 0.26$, $m_{\tilde{t}_1} = 250$ GeV, $\mu = 550$ GeV, $m_{\tilde{g}} = 600$ GeV, $A_t = A_b$, $m_{A^0} = 150$ GeV, and $M_{\tilde{D}} = 1.12 M_{\tilde{Q}}$. The solid lines correspond to the Yukawa-corrected decay widths, the dashed lines to the tree-level decay widths.

the region of the parameter μ where perturbation theory breaks down gets smaller (note that, in fact, the parameter range $|\mu| < 180$ GeV has been excluded by phenomenology at the CERN e^+e^- collider LEP and Tevatron [16,32]). There are many dips and peaks on the curves in Fig. 9(b), which come from the singularities at the threshold points. For example, at $\mu = -216$ GeV on the solid curve in Fig. 9(b), we have the threshold point $m_{\tilde{t}_2} = m_{\chi_4^0} + m_t$ for the decay into H^0.

In Figs. 10 and 11 we compare the results with the ones presented in earlier literature [9] where the $\mathcal{O}(\alpha_s)$ SUSY QCD corrections to the same three decay processes have been calculated. We present the tree-level decay widths and the Yukawa corrected decay widths as functions of $m_{\tilde{t}_2}$ and m_{A^0} in Figs. 10 and 11, respectively. For comparsion, we take the same input parameters as in Ref. [9]: $\tan\beta = 3$, $\cos\theta_{\tilde{t}} = 0.26$, $m_{\tilde{t}_1} = 250$ GeV, $m_{\tilde{g}} = 600$ GeV, $\mu = 550$ GeV in Figs. 10 and 11, and $m_{A^0} = 150$ GeV in Fig. 10, $m_{\tilde{t}_2} = 600$ GeV in Fig. 11. In both figures we assumed $M_{\tilde{D}} = 1.12 M_{\tilde{Q}}$. Our numerical results for the tree-level decay widths agree with the results of [9] except for a small difference, which is due to the running effects used in our calculation but not in Ref. [9]. The relative corrections in Fig. 10 vary from -22% to 26% for the decay into h^0, -60% to -4% for the decay into H^0, and -5% to 0% for the decay into A^0. The relative corrections in Fig. 11 vary from -1% to 23% for the decay into h^0, -24% to 60% for the decay into H^0, and -4% to -1% for the decay into A^0. After comparing with Figs. 3 and 5 in Ref. [9], we can see that the Yukawa corrections are comparable to the $\mathcal{O}(\alpha_s)$ SUSY QCD corrections for the decays into h^0 and H^0, but smaller than the $\mathcal{O}(\alpha_s)$ SUSY QCD corrections for the decays into A^0. There are two dips at $m_{A^0} = 348$ GeV and 352 GeV on the solid curve of the decay into h_0 in Fig. 11, which come from the singularities at the threshold points $m_{\tilde{t}_2} = m_{\tilde{t}_1} + m_{H^0}$.

Finally, in Fig. 12 we show the numerical improvement of the Yukawa corrections as a function of $\tan\beta$ in five methods of perturbative expansion: (i) the strict on-shell scheme (the dotted line), where the top quark pole mass 175.6 GeV, the bottom quark pole mass 4.25 GeV, the on-shell trilinear coupling A_t, and the Higgsino mass parameter μ were used, (ii) the improved scheme (the solid line), in which the QCD, SUSY QCD, and SUSY electroweak running quark masses $\hat{m}_q(Q)$ and the running trilinear coupling $\hat{A}_t(Q)$ were used, (iii) the complete improved scheme (the dashed line), in which the SUSY electroweak running parameter μ was also used as well as the same running parameters as in (ii), (iv) the $\hat{m}_t(Q)$ running scheme (the dash-dotted line), in which only the running top quark mass was used, and (v) the $\hat{m}_b(Q)$ running scheme (the dash-dot-dotted line), in which only the running bottom quark mass was used. Here we assumed $m_{\tilde{t}_1} = 250$ GeV, $M_2 = 200$ GeV, $A_t = A_b = 900$ GeV, $\mu = 200$ GeV, $m_{A^0} = 150$ GeV, and $M_{\tilde{Q}} = 1.5 M_{\tilde{U}} = 1.5 M_{\tilde{D}}$. One can see that the effect of the running of the top quark mass on the corrections cannot be neglected for low

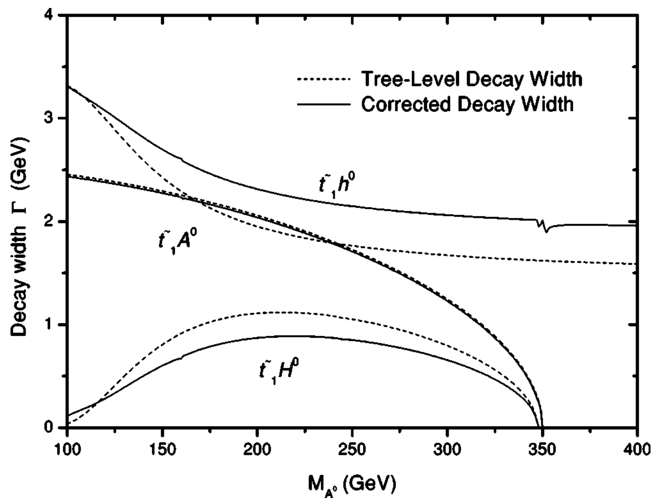

FIG. 11. The decay width of $\tilde{t}_2 \to \tilde{t}_1 H_i^0$ as a function of m_{A^0}, assuming $\tan\beta=3$, $\cos\theta_{\tilde{t}}=0.26$, $m_{\tilde{t}_1}=250$ GeV, $\mu=550$ GeV, $m_{\tilde{g}}=600$ GeV, $A_t=A_b$, and $M_{\tilde{D}}=1.12M_{\tilde{Q}}$. The solid lines correspond to the Yukawa-corrected decay widths, the dashed lines to the tree-level decay widths.

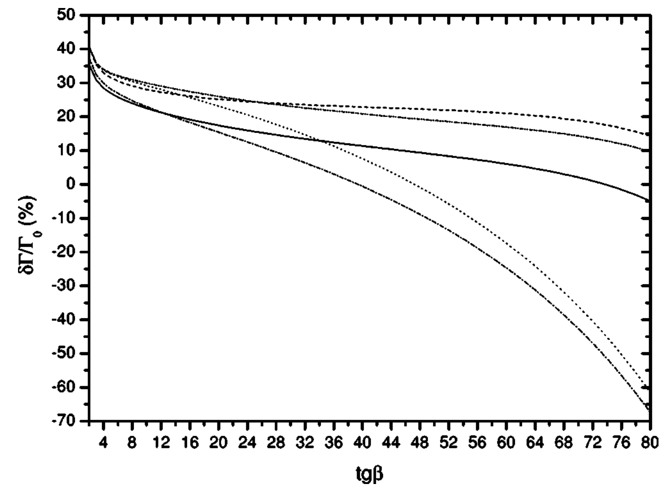

FIG. 12. The Yukawa corrections of $\tilde{t}_2 \to \tilde{t}_1 H^0$ as a function of $\tan\beta$, assuming $m_{\tilde{t}_1}=250$ GeV, $M_2=200$ GeV, $A_t=A_b=900$ GeV, $\mu=200$ GeV, $m_{A^0}=150$ GeV, and $M_{\tilde{Q}}=1.5M_{\tilde{U}}=1.5M_{\tilde{D}}$. The dotted line to the corrections using the on-shell parameters; the dashed line to the corrections using the running parameters $\hat{m}_t(Q)$, $\hat{m}_b(Q)$, $\hat{A}_t$, and $\hat{\mu}$; the solid line corresponds to the corrections using the same running parameters except the running $\hat{\mu}$; the dash-dotted line to the improved result only using the running mass $\hat{m}_t(Q)$; and the dash-dot-dotted line to the improved result only using the running mass $\hat{m}_b(Q)$.

$\tan\beta$ (<10), while the effect of the running of the bottom quark mass is quite significant for large $\tan\beta$ (>40). All the running effects with or without the running of the parameter μ make the convergence of the perturbation expansion much better. The relative corrections smoothly approach -5.0% and 14.3% with increasing $\tan\beta$ for the improved scheme and complete improved scheme, respectively, as shown by the solid line and the dashed line in Fig. 12.

In conclusion, we have calculated the Yukawa corrections to the widths of the heavier top squark decays into lighter top squarks and neutral Higgs bosons in the MSSM. These corrections depend on the masses of the neutral Higgs bosons and the lighter or heavier top squarks, and the parameter μ. For favorable parameter values, the corrections decrease or increase the tree-level decay widths significantly. In particular, for high values of $\tan\beta$ ($=30$) or low values of $\tan\beta$ ($=4$), the magnitudes of the corrections exceed at least 20% for the decay into h^0 and H^0, which is comparable to the $\mathcal{O}(\alpha_s)$ SUSY-QCD corrections. But for the decay into A^0, the corrections are smaller and the magnitudes are less than 10% in most of the parameter space. The numerical calculations also show that using the running quark masses and the running trilinear coupling A_t, which include the QCD, SUSY QCD, and SUSY electroweak effects, and resumming all high order ($\tan\beta$)-enhanced effects, can vastly improve the convergence of the perturbation expansion. We also discuss the effects of the running of the Higgsino mass parameter μ on the corrections, and find that they are significant, too, especially for large $\tan\beta$.

ACKNOWLEDGMENTS

This work was supported in part by the National Natural Science Foundation of China and the Doctoral Program Foundation of Higher Education of China.

APPENDIX A

The following couplings are given in order $O(h_t, h_b)$.

(1) Squark–squark–Higgs boson.

□□ (a) Squark–squark–h^0,

$$\hat{G}_1^{\tilde{q}} = \begin{pmatrix} -\sqrt{2}m_q h_q \begin{Bmatrix} c_\alpha \\ -s_\alpha \end{Bmatrix} & -\frac{1}{\sqrt{2}} h_q \left(A_q \begin{Bmatrix} c_\alpha \\ -s_\alpha \end{Bmatrix} + \mu \begin{Bmatrix} s_\alpha \\ -c_\alpha \end{Bmatrix} \right) \\ -\frac{1}{\sqrt{2}} h_q \left(A_q \begin{Bmatrix} c_\alpha \\ -s_\alpha \end{Bmatrix} + \mu \begin{Bmatrix} s_\alpha \\ -c_\alpha \end{Bmatrix} \right) & -\sqrt{2}m_q h_q \begin{Bmatrix} c_\alpha \\ -s_\alpha \end{Bmatrix} \end{pmatrix} \tag{A1}$$

for {up/down} type squarks, respectively. We use the abbreviations $s_\alpha=\sin\alpha$, $c_\alpha=\cos\alpha$. α is the mixing angle in the CP even neutral Higgs boson sector.

□□ (b) Squark-squark-H^0,

$$\hat{G}_2^{\tilde{q}}=\begin{pmatrix} -\sqrt{2}m_q h_q\begin{Bmatrix} s_\alpha \\ c_\alpha \end{Bmatrix} & -\frac{1}{\sqrt{2}}h_q\left(A_q\begin{Bmatrix} s_\alpha \\ c_\alpha \end{Bmatrix}-\mu\begin{Bmatrix} c_\alpha \\ s_\alpha \end{Bmatrix}\right) \\ -\frac{1}{\sqrt{2}}h_q\left(A_q\begin{Bmatrix} s_\alpha \\ c_\alpha \end{Bmatrix}-\mu\begin{Bmatrix} c_\alpha \\ s_\alpha \end{Bmatrix}\right) & -\sqrt{2}m_q h_q\begin{Bmatrix} s_\alpha \\ c_\alpha \end{Bmatrix} \end{pmatrix}. \tag{A2}$$

(c) Squark-squark-A^0,

$$\hat{G}_3^{\tilde{q}}=i\frac{gm_q}{2m_W}\begin{pmatrix} 0 & -A_q\begin{Bmatrix} \cot\beta \\ \tan\beta \end{Bmatrix}-\mu \\ A_q\begin{Bmatrix} \cot\beta \\ \tan\beta \end{Bmatrix}+\mu & 0 \end{pmatrix}. \tag{A3}$$

(d) Squark-squark-G^0,

$$\hat{G}_4^{\tilde{q}}=-i\frac{gm_q}{2m_W}\begin{pmatrix} 0 & -A_q+\mu\begin{Bmatrix} \cot\beta \\ \tan\beta \end{Bmatrix} \\ A_q-\mu\begin{Bmatrix} \cot\beta \\ \tan\beta \end{Bmatrix} & 0 \end{pmatrix}. \tag{A4}$$

(e) Squark-squark-$H^\pm$,

$$\hat{G}_5^{\tilde{b}}=(\hat{G}_5^{\tilde{t}})^T =\frac{g}{\sqrt{2}m_W}\begin{pmatrix} m_b^2\tan\beta+m_t^2\cot\beta & m_t(A_t\cot\beta+\mu) \\ m_b(A_b\tan\beta+\mu) & 2m_t m_b/\sin 2\beta \end{pmatrix}. \tag{A5}$$

(f) Squark-squark-$G^\pm$,

$$\hat{G}_6^{\tilde{b}}=(\hat{G}_6^{\tilde{t}})^T =\frac{-g}{\sqrt{2}m_W}\begin{pmatrix} m_t^2-m_b^2 & m_t(A_t-\mu\cot\beta) \\ m_b(\mu\tan\beta-A_b) & 0 \end{pmatrix}. \tag{A6}$$

2. Quark–quark–Higgs boson,

$$a_k^q=\left(\frac{1}{\sqrt{2}}h_q\begin{Bmatrix} -c_\alpha \\ s_\alpha \end{Bmatrix},-\frac{1}{\sqrt{2}}h_q\begin{Bmatrix} s_\alpha \\ c_\alpha \end{Bmatrix},\right.$$
$$-\frac{i}{\sqrt{2}}h_q\begin{Bmatrix} \cos\beta \\ \sin\beta \end{Bmatrix},\frac{-ig}{2m_W}\begin{Bmatrix} -m_t \\ m_b \end{Bmatrix},$$
$$\left.\begin{Bmatrix} h_b\sin\beta \\ h_t\cos\beta \end{Bmatrix},\frac{g}{\sqrt{2}m_W}\begin{Bmatrix} -m_b \\ m_t \end{Bmatrix}\right), \tag{A7}$$

$$b_k^q=\left(\frac{1}{\sqrt{2}}h_q\begin{Bmatrix} -c_\alpha \\ s_\alpha \end{Bmatrix},-\frac{1}{\sqrt{2}}h_q\begin{Bmatrix} s_\alpha \\ c_\alpha \end{Bmatrix},\right.$$
$$-\frac{i}{\sqrt{2}}h_q\begin{Bmatrix} \cos\beta \\ \sin\beta \end{Bmatrix},\frac{-ig}{2m_W}\begin{Bmatrix} m_t \\ -m_b \end{Bmatrix},$$
$$\left.h_q\begin{Bmatrix} \cos\beta \\ \sin\beta \end{Bmatrix},\frac{g}{\sqrt{2}m_W}\begin{Bmatrix} m_t \\ -m_b \end{Bmatrix}\right). \tag{A8}$$

3. Quark-squark-neutralino,

$$a_{ik}^{\tilde{q}}=-R_{i2}^{\tilde{q}}Y_q\begin{Bmatrix} N_{k4} \\ N_{k3} \end{Bmatrix}, \quad b_{ik}^{\tilde{q}}=-R_{i1}^{\tilde{q}}Y_q\begin{Bmatrix} N_{k4}^* \\ N_{k3}^* \end{Bmatrix}. \tag{A9}$$

Here N is the 4×4 unitary matrix diagonalizing the neutral gaugino-Higgsino mass matrix [2,31].

4. Quark-squark-chargino,

$$l_{ik}^{\tilde{q}}=R_{i2}^{\tilde{q}}Y_q\begin{Bmatrix} V_{k2} \\ U_{k2} \end{Bmatrix}, \quad k_{ik}^{\tilde{q}}=R_{i1}^{\tilde{q}}\begin{Bmatrix} Y_b U_{k2} \\ Y_t V_{k2} \end{Bmatrix}. \tag{A10}$$

Here U and V are the 2×2 unitary matrices diagonalizing the charged gaugino–Higgsino mass matrix [2,31].

5. Squark–squark–Higgs boson–Higgs boson.

(a) Squark-squark-H^--H_k ($k=1,2$),

$$\hat{G}_{5k}^{\tilde{b}}=(\hat{G}_{5k}^{\tilde{t}})^T=\frac{g^2}{2\sqrt{2}m_W^2}\begin{pmatrix} m_t^2 S_k+m_b^2 T_k & 0 \\ 0 & \frac{2m_t m_b}{\sin 2\beta}V_k \end{pmatrix} \tag{A11}$$

with

$$S_k=(\cos\alpha\cos\beta/\sin^2\beta, \quad \sin\alpha\cos\beta/\sin^2\beta), \tag{A12}$$

$$T_k=(-\sin\alpha\sin\beta/\cos^2\beta, \quad \cos\alpha\sin\beta/\cos^2\beta), \tag{A13}$$

$$V_k=(\sin(\beta-\alpha), \quad \cos(\beta-\alpha)). \tag{A14}$$

(b) Squark-squark-H^--H^+,

$$\hat{G}_{55}^{\tilde{q}}=\begin{pmatrix} -\begin{Bmatrix} h_b^2\sin^2\beta \\ h_t^2\cos^2\beta \end{Bmatrix} & 0 \\ 0 & -h_q^2\begin{Bmatrix} \cos^2\beta \\ \sin^2\beta \end{Bmatrix} \end{pmatrix}. \tag{A15}$$

(c) Squark-squark-H^--G^+,

$$\hat{G}^{\tilde{q}}_{56}=-\frac{g^2}{2m_W^2}\begin{pmatrix}\begin{Bmatrix}-m_b^2\tan\beta\\ m_t^2\cot\beta\end{Bmatrix} & 0\\ 0 & m_q^2\begin{Bmatrix}\cot\beta\\ -\tan\beta\end{Bmatrix}\end{pmatrix}. \tag{A16}$$

□□ (d) Squark-squark-G^--$H_k(k=1,2,3)$,

$$\hat{G}^{\tilde{b}}_{6k}=(\hat{G}^{\tilde{t}}_{6k})^T$$
$$=\frac{g^2}{2\sqrt{2}m_W^2}\begin{pmatrix}m_t^2SG_k+m_b^2TG_k & 0\\ 0 & 2m_tm_b/\sin 2\beta VG_k\end{pmatrix} \tag{A17}$$

with

$$SG_k=(\cos\alpha/\sin\beta,\quad \sin\alpha/\sin\beta,\quad i\cot\beta), \tag{A18}$$

$$TG_k=(\sin\alpha/\cos\beta,\quad -\cos\alpha/\cos\beta,\quad i\tan\beta), \tag{A19}$$

$$VG_k=(-\cos(\beta-\alpha),\quad \sin(\beta-\alpha),\quad -i). \tag{A20}$$

□□ (e) Squark-squark-H_k-$H_k(k=1,2,3)$,

$$\hat{G}^{\tilde{t}}_{kk}=\begin{pmatrix}\frac{-g^2}{2m_W^2}m_t^2D1_k & 0\\ 0 & \frac{-g^2}{2m_W^2}m_t^2D1_k\end{pmatrix} \tag{A21}$$

with

$$D1_k=(\sin^2\alpha/\sin^2\beta,\quad \cos^2\alpha/\sin^2\beta,\quad \cot^2\beta), \tag{A22}$$

$$\hat{G}^{\tilde{b}}_{kk}=\begin{pmatrix}\frac{-g^2}{2m_W^2}m_b^2D2_k & 0\\ 0 & \frac{-g^2}{2m_W^2}m_b^2D2_k\end{pmatrix} \tag{A23}$$

with

$$D2_k=(\cos^2\alpha/\sin^2\beta,\quad \sin^2\alpha/\sin^2\beta,\quad \tan^2\beta). \tag{A24}$$

□□ (f) Squark-squark-H^0-h^0,

$$\hat{G}^{\tilde{b}}_{12}=\begin{pmatrix}\frac{-g^2m_b^2\sin 2\alpha}{4m_W^2}D2 & 0\\ 0 & \frac{-g^2m_b^2\sin 2\alpha}{4m_W^2}D2\end{pmatrix} \tag{A25}$$

with $D2=-1/\cos^2\beta$,

$$\hat{G}^{\tilde{t}}_{12}=\begin{pmatrix}\frac{-g^2m_t^2\sin 2\alpha}{4m_W^2}D1 & 0\\ 0 & \frac{-g^2m_t^2\sin 2\alpha}{4m_W^2}D1\end{pmatrix} \tag{A26}$$

with $D1=-1/\sin^2\beta$.

□□ (g) Squark-squark-A^0-G^0,

$$\hat{G}^{\tilde{b}}_{35}=\begin{pmatrix}\frac{-g^2m_b^2\sin 2\beta}{4m_W^2}D2 & 0\\ 0 & \frac{-g^2m_b^2\sin 2\beta}{4m_W^2}D2\end{pmatrix}, \tag{A27}$$

$$\hat{G}^{\tilde{t}}_{35}=\begin{pmatrix}\frac{-g^2m_b^2\sin 2\beta}{4m_W^2}D1 & 0\\ 0 & \frac{-g^2m_b^2\sin 2\beta}{4m_W^2}D1\end{pmatrix}. \tag{A28}$$

Finally, we define $\hat{G}^{\tilde{q}}_{ji}=\hat{G}^{\tilde{q}}_{ij}$, and also $\hat{G}^{\tilde{q}}_{3(4)k}=0$, when $k=1,2,5$, i.e., there are no $A^0(G^0)h^0\tilde{q}\tilde{q}$, $A^0(G^0)H^0\tilde{q}\tilde{q}$, or $A^0(G^0)H^+\tilde{q}\tilde{q}$ couplings.

APPENDIX B

We define $q=t$ and b, q' the $SU(2)_L$ partner of q, and $q''=q$ for $k=1,\ldots,4$ and $q''=q'$ for $k=5,6$. Then we have

$$\frac{\delta m_W^2}{m_W^2}=\frac{g^2}{16\pi^2m_W^2}[m_b^2+m_t^2-A_0(m_t^2)-A_0(m_b^2)-m_t^2B_0-(m_t^2-m_b^2)B_1](m_W^2,m_b,m_t),$$

$$\frac{\delta m_Z^2}{m_Z^2}=\frac{3g^2}{8\pi^2m_W^2}\sum_{q=t,b}\Bigg\{\frac{1}{3}[(I_{3L}^q-e_q\sin^2\theta_W)^2+e_q^2\sin^4\theta_W][2m_q^2-2A_0(m_q^2)-m_q^2B_0]$$
$$-2m_q^2e_q\sin^2\theta_W(I_{3L}^q-e_q\sin^2\theta_W)B_0\Bigg\}(m_Z^2,m_q,m_q),$$

$$\delta Z_{H^-}=\frac{3g^2}{16\pi^2}[(m_t^2\cot^2\beta+m_b^2\tan^2\beta)(m_{H^+}^2G_1+B_1-m_t^2G_0)-2m_t^2m_b^2G_0](m_{H^+}^2,m_t,m_b)$$

$$+\frac{3}{16\pi^2}\sum_{i,j}(G_5^{\tilde{t}})_{ij}(G_5^{\tilde{t}})_{ij}G_0(m_{H^+}^2,m_{\tilde{t}_i},m_{\tilde{b}_j}),$$

$$\delta Z_{h^0}=\frac{3g^2m_t^2\cos^2\alpha}{16\pi^2m_W^2\sin^2\beta}(-2m_t^2G_0+B_1+m_h^2G_1)(m_{h_0}^2,m_t,m_t)+\frac{3g^2m_b^2\sin^2\alpha}{16\pi^2m_W^2\cos^2\beta}(-2m_b^2G_0+B_1+m_h^2G_1)(m_{h_0}^2,m_b,m_b)$$

$$+\frac{3}{16\pi^2}\sum_{i,j}(G_1^{\tilde{t}})_{ij}(G_1^{\tilde{t}})_{ij}G_0(m_{h_0}^2,m_{\tilde{t}_i},m_{\tilde{b}_j}),$$

$$\delta Z_{H^0}=\frac{3g^2m_t^2\sin^2\alpha}{16\pi^2m_W^2\sin^2\beta}(-2m_t^2G_0+B_1+m_H^2G_1)(m_{H_0}^2,m_t,m_t)+\frac{3g^2m_b^2\cos^2\alpha}{16\pi^2m_W^2\cos^2\beta}(-2m_b^2G_0+B_1+m_H^2G_1)(m_{H_0}^2,m_b,m_b)$$

$$+\frac{3}{16\pi^2}\sum_{i,j}(G_2^{\tilde{t}})_{ij}(G_2^{\tilde{t}})_{ij}G_0(m_{H_0}^2,m_{\tilde{t}_i},m_{\tilde{b}_j}),$$

$$\delta Z_{A^0}=\frac{3g^2m_t^2\cos^2\alpha}{16\pi^2m_W^2\sin^2\beta}(-2m_t^2G_0+B_1+m_h^2G_1)(m_{A_0}^2,m_t,m_t)+\frac{3g^2m_b^2\sin^2\alpha}{16\pi^2m_W^2\cos^2\beta}(-2m_b^2G_0+B_1+m_h^2G_1)(m_{A_0}^2,m_b,m_b)$$

$$+\frac{3}{16\pi^2}\sum_{i,j}(G_3^{\tilde{t}})_{ij}(G_3^{\tilde{t}})_{ij}G_0(m_{A_0}^2,m_{\tilde{t}_i},m_{\tilde{b}_j}),$$

$$T_{H_k}=\frac{-3gm_t^2}{8\pi^2m_W\sin\beta}A_0(m_t^2)+\frac{-3gm_b^2}{8\pi^2m_W\cos\beta}A_0(m_b^2)-\sum_{q=t,b}\sum_j(G_k^{\tilde{q}})_{jj}A_0(m_{\tilde{q}_j}^2),$$

$$\Sigma_{GH}=-\frac{3g^2}{16\pi^2m_W^2}(m_t^2\cot\beta-m_b^2\tan\beta)[m_t^2B_0+A_0(m_b^2)+m_{H^+}^2B_1]+m_t^2m_b^2(\tan\beta-\cot\beta)B_0(m_{H^+}^2,m_t,m_b)$$

$$+\frac{-3}{16\pi^2}\sum_{j,l}(G_5^{\tilde{t}})_{jl}(G_6^{\tilde{t}})_{lj}B_0(m_{H^+}^2,m_{\tilde{t}_l},m_{\tilde{b}_j})+\frac{3}{16\pi^2}\sum_{q=t,b}\sum_j i(G_{56}^{\tilde{q}})_{jj}A_0(m_{\tilde{q}_j}^2),$$

$$\frac{\delta m_t}{m_t}=\frac{1}{16\pi^2}\sum_{k=1}^{6}\left[\frac{m_{t''}}{m_t}a_k^ta_k^{t''}B_0-\frac{1}{2}(a_k^tb_k^{t''}+b_k^ta_k^{t''})B_1\right](m_t^2,m_{t''},m_{H_k})$$

$$+\frac{g^2}{16\pi^2}\sum_{k=1}^{4}\sum_j\left[\frac{m_{\tilde{\chi}_k^0}}{m_t}a_{jk}^{\tilde{t}}b_{jk}^{\tilde{t}*}B_0+\frac{1}{2}(|a_{jk}^{\tilde{t}}|^2+|b_{jk}^{\tilde{t}}|^2)(B_0+B_1)\right](m_t^2,m_{\tilde{t}_j},m_{\tilde{\chi}_k^0})$$

$$+\frac{g^2}{16\pi^2}\sum_{k=1}^{2}\sum_j\left[\frac{m_{\tilde{\chi}_k^+}}{m_b}l_{jk}^{\tilde{b}}k_{jk}^{\tilde{b}}B_0+\frac{1}{2}(|l_{jk}^{\tilde{b}}|^2+|k_{jk}^{\tilde{b}}|^2)(B_0+B_1)\right](m_t^2,m_{\tilde{b}_j},m_{\tilde{\chi}_k^+}),$$

$$\delta m_{\tilde{t}_i}^2=\frac{1}{16\pi^2}\Bigg\{\sum_{k=1}^{6}\sum_j(G_k^{\tilde{t}})_{ij}(G_k^{\tilde{t}''})_{ji}B_0(m_{\tilde{t}_i}^2,m_{\tilde{t}_j''},m_{H_k})-2g^2\sum_{k=1}^{4}\{(|a_{ik}^{\tilde{t}}|^2+|b_{ik}^{\tilde{t}}|^2)[m_{\tilde{t}_i}^2B_1+A_0(m_{\tilde{\chi}_k^0}^2)+m_t^2B_0]$$

$$+2m_tm_{\tilde{\chi}_k^0}\,\mathrm{Re}(a_{ik}^{\tilde{t}}b_{ik}^{\tilde{t}*})B_0\}(m_{\tilde{t}_i}^2,m_t,m_{\tilde{\chi}_k^0})-2g^2\sum_{k=1}^{2}\{(|l_{ik}^{\tilde{t}}|^2+|k_{ik}^{\tilde{t}}|^2)[m_{\tilde{t}_i'}^2B_1+A_0(m_{\tilde{\chi}_k^+}^2)+m_{t'}^2B_0]$$

$$+2m_{t'}m_{\tilde{\chi}_k^+}\mathrm{Re}(l_{ik}^{\tilde{t}}k_{ik}^{\tilde{t}*})B_0\}(m_{\tilde{t}_i}^2,m_{t'},m_{\tilde{\chi}_k^+})\Bigg\},$$

$$\delta Z_{\tilde{t}_i}=\frac{1}{16\pi^2}\Bigg\{\sum_{k=1}^{6}\sum_{j}(G_k^{\tilde{t}})_{ij}(G_k^{\tilde{t}''})_{ji}G_0(m_{\tilde{t}_i}^2,m_{\tilde{t}_j''},m_{H_k})+2g^2\sum_{k=1}^{4}[(|a_{ik}^{\tilde{t}}|^2+|b_{ik}^{\tilde{t}}|^2)(B_1+m_{\tilde{t}_i}^2G_1-m_t^2G_0)$$
$$-2m_tm_{\tilde{\chi}_k^0}\mathrm{Re}(a_{ik}^{\tilde{t}}b_{ik}^{\tilde{t}*})G_0](m_{\tilde{t}_i}^2,m_t,m_{\tilde{\chi}_k^0})+2g^2\sum_{k=1}^{2}[(|l_{ik}^{\tilde{t}}|^2+|k_{ik}^{\tilde{t}}|^2)(B_1+m_{\tilde{t}_i'}^2G_1-m_{t'}^2G_0)$$
$$-2m_{q'}m_{\tilde{\chi}_k^+}\mathrm{Re}(l_{ik}^{\tilde{q}}k_{ik}^{\tilde{q}*})G_0](m_{\tilde{q}_i}^2,m_{q'},m_{\tilde{\chi}_k^+})\Bigg\},$$

$$\Sigma_{Hh}(p^2)=\frac{-3g^2m_t^2\sin 2\alpha}{32\pi^2m_W^2\sin^2\beta}[(2m_t^2B_0+p^2B_1)(p^2,m_t,m_t)+A_0(m_t^2)]$$
$$+\frac{3g^2m_b^2\sin 2\alpha}{32\pi^2m_W^2\cos^2\beta}[(2m_b^2B_0+p^2B_1)(p^2,m_b,m_b)+A_0(m_b^2)]$$
$$+\frac{3}{16\pi^2}\sum_q\sum_{i,j}(G_1^{\tilde{q}})_{ji}(G_2^{\tilde{q}})_{ij}B_0(p^2,m_{\tilde{q}_j},m_{\tilde{q}_i})+\frac{3i}{16\pi^2}\sum_q\sum_i(G_{12}^{\tilde{q}})_{ii}A_0(m_{\tilde{q}_i}),$$

$$\delta Z_{H^0h^0}=\frac{\Sigma_{Hh}(h_0^2)}{m_{H^0}^2-m_{h^0}^2},\qquad \delta Z_{h^0H^0}=\frac{\Sigma_{Hh}(H_0^2)}{m_{h^0}^2-m_{H^0}^2},$$

$$\Sigma_{12}^{\tilde{t}}(p^2)=\frac{1}{16\pi^2}\Bigg\{\sum_{k=1}^{6}\sum_j(G_k^{\tilde{t}})_{1j}(G_k^{\tilde{t}''})_{j2}B_0(p^2,m_{\tilde{t}_j''},m_{H_k})-2g^2\sum_{k=1}^{4}\{(a_{1k}^{\tilde{t}}a_{2k}^{\tilde{t}*}+b_{1k}^{\tilde{t}}b_{2k}^{\tilde{t}*})[p^2B_1+A_0(m_{\tilde{\chi}_k^0}^2)+m_t^2B_0]$$
$$+m_tm_{\tilde{\chi}_k^0}(a_{1k}^{\tilde{t}}b_{2k}^{\tilde{t}*}+a_{2k}^{\tilde{t}*}b_{1k}^{\tilde{t}})B_0\}(p^2,m_t,m_{\tilde{\chi}_k^0})-2g^2\sum_{k=1}^{2}\{(l_{1k}^{\tilde{t}}l_{2k}^{\tilde{t}*}+k_{1k}^{\tilde{t}}k_{2k}^{\tilde{t}*})[p^2B_1+A_0(m_{\tilde{\chi}_k^+}^2)+m_{t'}^2B_0]$$
$$+m_{t'}m_{\tilde{\chi}_k^+}(l_{1k}^{\tilde{t}}k_{2k}^{\tilde{t}*}+l_{2k}^{\tilde{t}*}k_{1k}^{\tilde{t}})B_0\}(p^2,m_{t'},m_{\tilde{\chi}_k^+})\Bigg\},$$

$$\delta\theta_{\tilde{t}}+\delta Z_{21}^{\tilde{t}}=\frac{1}{2(m_{\tilde{t}_1}^2-m_{\tilde{t}_2}^2)}[\Sigma_{12}^{\tilde{t}}(m_{\tilde{t}_2}^2)-\Sigma_{12}^{\tilde{t}}(m_{\tilde{t}_1}^2)],$$

$$\Pi_{ij}^L(p^2)=-\frac{3}{16\pi^2}\sum_{k=1}^{2}[l_{ki}^{\tilde{t}}l_{kj}^{\tilde{t}}B_1(p^2,m_b,m_{\tilde{t}_k})+k_{ki}^{\tilde{b}}k_{kj}^{\tilde{b}}B_1(p^2,m_t,m_{\tilde{b}_k})],$$

$$\Pi_{ij}^R(p^2)=-\frac{3}{16\pi^2}\sum_{k=1}^{2}[k_{ki}^{\tilde{t}}k_{kj}^{\tilde{t}}B_1(p^2,m_b,m_{\tilde{t}_k})+l_{ki}^{\tilde{b}}l_{kj}^{\tilde{b}}B_1(p^2,m_t,m_{\tilde{b}_k})],$$

$$\Pi_{ij}^{S,L}(p^2)=\frac{3}{16\pi^2}\sum_{k=1}^{2}[m_bk_{ki}^{\tilde{t}}l_{kj}^{\tilde{t}}B_0(p^2,m_b,m_{\tilde{t}_k})+m_tl_{ki}^{\tilde{b}}k_{kj}^{\tilde{b}}B_0(p^2,m_t,m_{\tilde{b}_k})],$$

$$\Pi_{ij}^{S,R}(p^2)=\frac{3}{16\pi^2}\sum_{k=1}^{2}[m_bl_{ki}^{\tilde{t}}k_{kj}^{\tilde{t}}B_0(p^2,m_b,m_{\tilde{t}_k})+m_tk_{ki}^{\tilde{b}}l_{kj}^{\tilde{b}}B_0(p^2,m_t,m_{\tilde{b}_k})].$$

Here A_0 and B_1 are also as defined by Passarino and Veltman [20], except we work in the metric $(1,-1,-1,-1)$, and $G_1=\partial B_1/\partial p^2$, $G_0=-\partial B_0/\partial p^2$.

[1] H. P. Nilles, Phys. Rep. **110**, 1 (1984); A. B. Lahanas and D. V. Nanopoulos, *ibid.* **145**, 1 (1987); *Supersymmetry*, edited by S. Ferrara (North Holland/World Scientific, Singapore, 1987), Vols. 1 and 2.

[2] H. E. Haber and G. L. Kane, Phys. Rep. **117**, 75 (1985).

[3] Atlas Collaboration, A. Airapetian *et al.*, Atlas Technical Design Report No. CERN/LHCC/99-14/15; CMS Collaboration, M. Della Negra *et al.*, CMS Technical Proposal No. CERN/LHCC/94-38; F. Gianotti, in *Proceedings of the IVth International Symposium on Radiative Corrections (RADCOR 98)*, edited by J. Solá (World Scientific, Singapore, 1999), p. 270.

[4] D. J. Miller, in *Proceedings of the IVth International Symposium on Radiative Corrections (RADCOR 98)* (Ref. [3]), p. 289.

[5] H. Baer, V. Barger, D. Karatas, and X. Tata, Phys. Rev. D **36**, 96 (1987); K. Hikasa and M. Kobayashi, *ibid.* **36**, 724 (1987); R. M. Barnett, J. F. Gunion, and H. E. Haber, *ibid.* **37**, 1892 (1988); H. Baer, X. Tata, and J. Woodside, *ibid.* **42**, 1568 (1990); K. Hikasa and M. Drees, Phys. Lett. B **252**, 127 (1990); A. Bartl, W. Majerotto, B. Mösslacher, and N. Oshimo, Z. Phys. C **52**, 477 (1991); A. Bartl, W. Majerotto, and W. Porod, *ibid.* **64**, 499 (1994); **68**, 518(E) (1995).

[6] A. Bartl, H. Eberl, K. Hidaka, S. Kraml, T. Kon, W. Majerotto, W. Porod, and Y. Yamada, Phys. Lett. B **435**, 118 (1998).

[7] K. Hidaka and A. Bartl, Phys. Lett. B **501**, 78 (2001).

[8] S. Kraml, H. Eberl, A. Bartl, W. Majerotto, and W. Porod, Phys. Lett. B **386**, 175 (1996); A. Djouadi, W. Hollik, and C. Jünger, Phys. Rev. D **55**, 6975 (1997).

[9] A. Bartl, H. Eberl, K. Hidaka, S. Kraml, W. Majerotto, W. Porod, and Y. Yamada, Phys. Lett. B **419**, 243 (1998).

[10] J. Guasch, W. Hollik, and J. Solá, Phys. Lett. B **437**, 88 (1998).

[11] J. Guasch, W. Hollik, and J. Solá, Phys. Lett. B **510**, 211 (2001).

[12] Hou Hong-Sheng, Ma Wen-Gan, Wan Lang-Hui, and Zhang Ren-You, Phys. Rev. D **65**, 075019 (2002).

[13] Li Lin Yang, Chong Sheng Li, and Qiang Li, Report No. PKU-TH-0206022.

[14] A. Bartl, H. Eberl, K. Hidaka, S. Kraml, W. Majerotto, W. Porod, and Y. Yamada, Phys. Lett. B **419**, 243 (1998); Phys. Rev. D **59**, 115007 (1999).

[15] Li Gang Jin and Chong Sheng Li, Phys. Rev. D **65**, 035007 (2001).

[16] H. Eberl, *et al.*, Phys. Rev. D **62**, 055006 (2000).

[17] S. Sirlin, Phys. Rev. D **22**, 971 (1980); W. J. Marciano and A. Sirlin, *ibid.* **22**, 2695 (1980); **31**, 213(E) (1985); A. Sirlin and W. J. Marciano, Nucl. Phys. **B189**, 442 (1981); K. I. Aoki *et al.*, Prog. Theor. Phys. Suppl. **73**, 1 (1982).

[18] R. Santos and A. Barroso, Phys. Rev. D **56**, 5366 (1997).

[19] A. Mendez and A. Pomarol, Phys. Lett. B **279**, 98 (1992).

[20] G. Passarino and M. Veltman, Nucl. Phys. **B160**, 151 (1979).

[21] A. Bartl, H. Eberl, K. Hidaka, T. Kon, W. Majerotto, and Y. Yamada, Phys. Lett. B **402**, 303 (1997).

[22] D. Pierce and A. Papadopoulos, Phys. Rev. D **50**, 565 (1994).

[23] H. Eberl, M. Kincel, W. Majerotto, and Y. Yamada, Phys. Rev. D **64**, 115013 (2001).

[24] Particle Data Group, D. Groom *et al.*, Eur. Phys. J. C **3**, 1 (1998).

[25] M. Carena, D. Garcia, U. Nierste, and C. E. M. Wagner, Nucl. Phys. **B577**, 88 (2000).

[26] Damien M. Pierce, Jonathan A. Bagger, and Ren Jie Zhang, Nucl. Phys. **B491**, 3 (1997).

[27] M. Beneke and A. Signer, Phys. Lett. B **471**, 233 (1999); A. H. Hoang, Phys. Rev. D **61**, 034005 (2000).

[28] S. G. Gorishny, A. L. Kataev, S. A. Larin, and L. R. Surguladze, Mod. Phys. Lett. A **5**, 2703 (1990); Phys. Rev. D **43**, 1633 (1991); A. Djouadi, M. Spira, and P. M. Zerwas, Z. Phys. C **70**, 427 (1996); A. Djouadi, J. Kalinowski, and M. Spira, Comput. Phys. Commun. **108**, 56 (1998); M. Spira, Fortschr. Phys. **46**, 203 (1998).

[29] M. Carena, M. Quirós, and C. E. M. Wagner, Nucl. Phys. **B461**, 407 (1996).

[30] Damien M. Pierce, 1997 TASI lectures, hep-ph/9805497.

[31] P. Nath, R. Arnowitt, and A. Chamseddine, *Applied* $N=1$ *Supergravity*, ICTP series in Theoretical Physics (World Scientific, Singapore, 1984); J. F. Gunion and H. E. Haber, Nucl. Phys. **B272**, 1 (1986); L. E. Ibáñez and G. G. Ross, in *Perspectives on Higgs Physics*, edited by G. L. Kane (World Scientific, Singapore, 1993), hep-ph/9204201.

[32] A. Savoy-Navarro, talk at the International Europhysics Conference on High Energy Physics (HEP99), 1999, Tampere, Finland. For transparencies see http://neutrino.pc.helsinki.fi/hep99/Transparencies/session-07/Savoy-Navarro.pdf